THE JOURNAL OF PHYSICAL CHEMISTRY B

Article

pubs.acs.org/JPCB

# Liquid–Liquid Extraction of Uranyl by TBP: The TBP and Ions Models and Related Interfacial Features Revisited by MD and PMF Simulations

G. Benay and G. Wipff*

Laboratoire MSM, UMR 7177, Institut de Chimie, 1 rue B. Pascal, 67000 Strasbourg, France

Supporting Information

**ABSTRACT:** We report a molecular dynamics (MD) study of biphasic systems involved in the liquid–liquid extraction of uranyl nitrate by tri-*n*-butylphosphate (TBP) to hexane, from "pH neutral" or acidic (3 M nitric acid) aqueous solutions, to assess the model dependence of the surface activity and partitioning of TBP alone, of its $UO_2(NO_3)_2(TBP)_2$ complex, and of $UO_2(NO_3)_2$ or $UO_2^{2+}$ uncomplexed. For this purpose, we first compare several electrostatic representations of TBP with regards to its polarity and conformational properties, its interactions with $H_2O$, $HNO_3$, and $UO_2(NO_3)_2$ species, its relative free energies of solvation in water or oil environments, the properties of the pure TBP liquid and of the pure-TBP/water interface. The free energies of transfer of TBP, $UO_2(NO_3)_2$, $UO_2^{2+}$, and the $UO_2(NO_3)_2(TBP)_2$ complex across the water/oil interface are then investigated by potential of mean force (PMF) calculations, comparing different TBP models and two charge models of uranyl nitrate. Describing uranyl and nitrate ions with integer charges (+2 and −1, respectively) is shown to exaggerate the hydrophilicity and surface activity of the $UO_2(NO_3)_2(TBP)_2$ complex. With more appropriate ESP charges, mimicking charge transfer and polarization effects in the $UO_2(NO_3)_2$ moiety or in the whole complex, the latter is no more surface active. This feature is confirmed by MD, PMF, and mixing–demixing simulations with or without polarization. Furthermore, with ESP charges, pulling the $UO_2(NO_3)_2$ species to the TBP phase affords the formation of $UO_2(NO_3)_2(TBP)_2$ at the interface, followed by its energetically favorable extraction. The neutral complexes should therefore not accumulate at the interface during the extraction process, but diffuse to the oil phase. A similar feature is found for an $UO_2(NO_3)_2(Amide)_2$ neutral complex with fatty amide extracting ligands, calling for further simulations and experimental studies (e.g., time evolution of the nonlinear spectroscopic signature and of surface tension) on the interfacial landscape upon ion extraction.

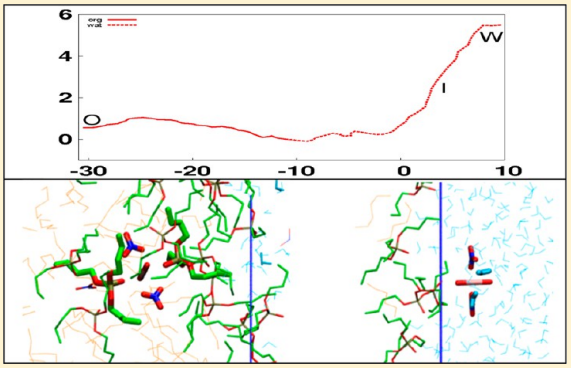


## INTRODUCTION

What happens at the water–"oil" interface is of capital importance in many fields like solvent extraction,[1,2] interfacial nanochemistry,[3] electrochemistry,[4] biphasic catalysis,[5] drug delivery, or biological processes.[6,7] The question also arises upon ion separation and purification by liquid–liquid extraction, where hydrophilic cations are transferred to an "oil" phase after being complexed by hydrophobic ligands.[8] The $U^{(VI)}$ uranium and $Pu^{(IV)}$ plutonium separation from acidic solutions obtained by dissolution of irradiated fuel is a particularly important case. It is the cornerstone of the nuclear waste partitioning and reprocessing (PUREX process)[9] and represents a much studied prototype for a broad class of cation separation reactions by neutral extractants. In that process the source phase containing, among others, uranyl nitrate dissolved in nitric acid, is contacted with the receiving phase (≈30% of tri-*n*-butylphosphate (TBP) dissolved in aliphatic solvent like kerosene). After mixing and separation (for instance, using mixer-settler units to obtain a continuous process), one progressively obtains an oil-rich phase into which the $UO_2(NO_3)_2(TBP)_2$ complex is extracted.[10] The overall reaction is

$$(UO_2^{2+})_{aq} + 2(NO_3^-)_{aq} + 2(TBP)_{oil} \rightarrow ? ? ?$$
$$\rightarrow [UO_2(NO_3)_2(TBP)_2]_{oil}$$

In the source phase $UO_2^{2+}$ is mainly hydrated, forming $UO_2(H_2O)_5^{2+}$ or mixed $UO_2(H_2O)_m(NO_3)_n^{2-n}$ species, depending on the nitric acid concentration. Intermediate stages of the extraction process have not been characterized but, based on kinetic studies on model systems using for instance the capillary cell,[11] the single drop[12] or stirred-cell[13] techniques, it has been proposed that the uranyl complexation reaction occurs "at the interface",[14,15] as for many other metal extraction systems,[16−22] without defining, however, the size, composition

**Received:** November 18, 2013
**Revised:** February 19, 2014
**Published:** February 20, 2014

   dx.doi.org/10.1021/jp411332e | *J. Phys. Chem. B* 2014, 118, 3133−3149

and characteristics of "the interface". Insights might be in principle obtained experimentally by nonlinear spectroscopic techniques,[7,23] but the latter remain to be developed for interfaces "in action", as involved in complex heterogeneous extraction systems.[24] On the other hand, our understanding of the structure of aqueous interfaces has benefited from the application of theoretical approaches. Molecular dynamics "MD" simulations afforded nanoscopic representations of neat water−oil interfaces[25] and of electrolyte distributions at aqueous surfaces.[26−28] Our group focused on assisted ion extraction and transport in supramolecular chemistry, involving extractants (crown ethers, cryptands, calixarenes, acyclic O- or N-ligands), ions and their complexes.[29−33] Regarding uranyl extraction, it was found that the $UO_2(NO_3)_2(TBP)_2$ complex, although hydrophobic, prefers the interface over the oil phase, like TBP itself.[34−37] Furthermore, in mixing−demixing MD simulations of water/oil "random" mixtures (oil = $CHCl_3$ or SC−$CO_2$) containing the undissociated $UO_2(NO_3)_2$ salt and concentrated TBP, the $UO_2(NO_3)_2(TBP)_2$ or $UO_2(NO_3)_2(TBP)(H_2O)$ complexes formed spontaneously and adsorbed at the interface with either pH neutral or acidic water.[38,39] The surface activity of $UO_2(NO_3)_2(TBP)_2$ was supported by subsequent PMF (potential of mean force) simulations of Jayasinghe and Beck.[40] They found that the corresponding free energy profile across the neutral TBP +hexane/water interface displays a minimum with respect to the oil phase, ranging from ≈6 to 3 kcal/mol, depending on the TBP concentration. Note that these results have been obtained with classical force field representations of the potential energy, where intermolecular forces are presented by pairwise additive interactions, using fixed atomic charges to depict Coulombic interactions, thus without accounting for nonadditivity effects. Furthermore, most simulations (except ref 41) used MNDO charges on TBP from the literature[34] and integer charges on uranyl and nitrate moieties of $UO_2(NO_3)_2$, free or complexed by TBP.

In this paper we revisit the uranyl nitrate extraction by TBP from aqueous solutions (neutral or with 3 M nitric acid) and investigate several computational issues that can have deep consequences regarding the interfacial landscape in the extraction process. (i) First, the TBP model. It determines the TBP conformation and polarity, and thus the properties of the pure liquid (structure, dipole moments, diffusion coefficients)[42] or H-bonding interactions with water and acid molecules,[43] thereby affecting its calculated surface properties and complexing ability toward uranyl. We thus consider different sets of TBP charges and compare previous results obtained with the MNDO model to those obtained with other QM derived models. (ii) The electrostatic representation of the extracted salt: how important is the charge transfer from $NO_3^-$ to $UO_2^{2+}$ in the $UO_2(NO_3)_2$ moiety ? The charge transferability of ions upon complexation or pairing with counterions, generally assumed for convenience, is questionable. For example, modeling ionic liquids with reduced instead of integer charges improves their simulated properties.[44] Scaling down the ionic charges is also a simple and practical way to model ionic interactions in water.[45] We thus decided to compare two models of the uranyl nitrate moiety (noted in short "UN"), in its uncomplexed $UO_2(NO_3)_2$ or complexed $UO_2(NO_3)_2(TBP)_2$ states: in the first model, labeled $UN_{integer}$, uranyl and nitrate bear integer (+2 and −1) charges, whereas in the second model, labeled $UN_{ESP}$, the atomic charges have been fitted on the $UO_2(NO_3)_2$ "complex", thus accounting for electron redistribution. (iii) Polarization effects. The latter can be quite significant, e.g., upon TBP or anion binding to hard cations, or to depict aqueous surfaces that are less polar than the bulk water.[46] They have been shown to influence the distribution of electrolytes at interfaces[47,48] and to improve the representation of salts of *f*-ions (for instance lanthanide nitrates) in solution[49] or of ionic melts.[50,51] We thus compare, for selected systems, MD results without polarization and with added atomic polarizabilities on solutes, in conjunction with polarizable models for water and oil.

More specifically, we first describe different TBP electrostatic models with regards to the TBP "polarity" and its impact for the assisted extraction process. We then consider the neat biphasic systems (without uranyl nitrate) to gain insights into the characteristics of the interface and the "humidity" of the oil phase, in acidic and neutral conditions. Then, following previous related PMF studies,[40,52−54] we explore the energetics of interface crossing by the most relevant species (the free TBP ligand, its $UO_2(NO_3)_2(TBP)_2$ complex, $UO_2(NO_3)_2$ or $UO_2^{2+}$ uncomplexed), by calculating the corresponding free energy profiles with different models in pH neutral and, in some cases, in acidic conditions. Finally, we report mixing-demixing experiments of "random" mixtures of water, TBP, hexane solvents and complexes, to assess their partitioning after phase separation, with different models. Beyond computational issues, our paper aims at improving the description of the molecular composition and structure of the interface, in order to better understand the complexation and extraction mechanism.

## METHODS

**MD Simulations of Biphasic Solutions.** Molecular dynamics simulations were performed with the AMBER10 software[55] with the following representation of the potential energy *U*:

$$U = \sum_{\text{bonds}} k_l(l - l_0)^2 + \sum_{\text{angles}} k_\theta(\theta - \theta_\theta)^2 + \sum_{\text{dihedrals}} \sum_n V_n(1 + \cos(n\varphi - \gamma)) + \sum_{i<j} \left[ \frac{q_i q_i}{R_{ij}} - 2\varepsilon_{ij}\left(\frac{R^*_{ij}}{R_{ij}}\right)^6 + \varepsilon_{ij}\left(\frac{R^*_{ij}}{R_{ij}}\right)^{12} \right]$$

It accounts for the deformation of bonds, angles, dihedral angles, electrostatic and van der Waals interactions (assumed to be pairwise additive in this 1−6−12 potential). The $CH_2$ and $CH_3$ groups of TBP and hexane were represented in the united atom approximation, using the Cornell et al. force field parameters.[56] The solvents were represented explicitly, using the TIP3P water[57] and OPLS hexane[58] models without polarization ("NO-POL" models). The 1−4 van der Waals and Coulombic interactions were divided by 8.0 and 1.2, respectively. For uranyl nitrate, we compared two sets of charges, labeled $UN_{integer}$ and $UN_{ESP}$, respectively, using the same 6−12 parameters as in previous work.[59] In the $UN_{integer}$ model, uranyl and nitrate bear integer charges ($q_{UO2}$ = +2.0 and $q_{NO3}$ = −1.0 e) and the uranyl atomic charges ($q_U$ = +2.5, $q_O$ = −0.25 e)[59] are the same as those recently developed from QM approaches.[60] The $UN_{ESP}$ charges were obtained from ESP calculations (Merz−Kollman procedure implemented in Gaussian09) on $UO_2(NO_3)_2$, yielding ions charges of $q_{UO2}$ = +1.069 and $q_{NO3}$ = −0.534 e (see Table S1 for a summary of


dx.doi.org/10.1021/jp411332e | J. Phys. Chem. B 2014, 118, 3133−3149

**Table 1. Characteristics of the Simulated Systems**

| | label | solute(s) | $N_{hexane}$ | water | box size $x^*y^*(z_{oil} + z_{wat})$ (Å$^3$) | time (ns)[a] |
|---|---|---|---|---|---|---|
| | **A** | 143 TBP | 0 | 0 | 39 × 39 × 39 | 2 ; (2)[b] |
| | **B** | 289 TBP | 0 | 2109 $H_2O$ | 40 × 40 × (84 + 35) | 10 ; ($5^a$ +$5^b$) |
| | **C** | 106 TBP[c] | 530 | 2113 $H_2O$ | 40 × 40 × (100 + 39) | 5 ; (+2)[b]; (+$1^d$ +5)[a] |
| | **D** | 106 TBP[e] | 530 | 20 "acid"[f] | 38 × 38 × (100 + 35) | 5 ; (+2)[b]; (+$1^d$ +5)[a] |
| | **E** | 100 TBP[g] | 320 | 2103 $H_2O$ | 37 × 37 × (80 + 48) | 5 |
| | **F** | 99 TBP | 315 | 20 "acid"[f] | 35 × 35 × (88 + 37) | 5 |
| | **G** | 5 $UO_2(NO_3)_2(TBP)_2$ + 106 TBP | 530 | 2114 $H_2O$ | 40 × 40 × (99 + 41) | 5 ; (5)[b] |
| PMF | **H** | 1 TBP | 302 | 2104 $H_2O$ | 40 × 40 × (39 + 41) | $1^h$ + 60 ; ($1^h$ +60)[b] |
| | **I** | 1 TBP + 105 TBP | 530 | 2113 $H_2O$ | 40 × 40 × (100 + 39) | $2^h$ + 60 |
| | **J** | 1 $UO_2(NO_3)_2(TBP)_2$ +104 TBP | 520 | 2090 $H_2O$ | 40 × 40 × (100 + 39) | $1^h$ + 60 |
| | **K** | 1 $UO_2(NO_3)_2(TBP)_2$ +104 TBP | 520 | 20 "acid"[f] | 38 × 38 × (106 + 29) | $1^h$ + 60 |
| | **L** | 1 $UO_2(NO_3)_2(TBP)_2$ +99 TBP[g] | 315 | 2125 $H_2O$ | 37 × 37 × (79 + 50) | $5^{a,h}$ +$1^{b,h}$ + $60^b$ |
| | **M** | 1 $UO_2(NO_3)_2$ + 104 TBP | 520 | 2117 $H_2O$ | 40 × 40 × (100 + 39) | $2^h$ + 60 |
| | **N** | 1 $UO_2^{2+}$ + 2 $NO_3^-$ + 104 TBP | 520 | 2123 $H_2O$ | 40 × 40 × (100 + 39) | $1^h$ + 60 |
| | **O** | 1 $UO_2^{2+}$ + 2 $NO_3^-$ + 106 TBP | 530 | 19 "acid"[f] | 38 × 38 × (109 + 25) | $1^h$ + 60 |
| | **P** | 1 $UO_2(NO_3)_2$ + 4 $UO_2(NO_3)_2$ | 302 | 2048 $H_2O$ | 40 × 40 × (42 + 38) | $2^h$ + 60 |

[a]Simulations "NO-POL" without polarization, unless otherwise specified. [b]Simulation with polarization ("POL" model). [c]1.1 M TBP, 30 vol% TBP in hexane, including interfaces. [d]Simulation at a temperature of 400 K. [e]1.2 M TBP, 33 vol% TBP in hexane, including interfaces. [f]"acid" = 3 $NO_3^-$ + 3 $H_3O^+$ + 1 $HNO_3$ + 62 $H_2O$, to obtain 3 M nitric acid with 75% dissociation. [g]1.5 M TBP, 41 vol% TBP in hexane, including interfaces [h]Equilibration time before starting the PMF for at least 60 ns.

the different UN models). Charges on TBP were likewise obtained from QM calculations at the DFT or HF levels with different basis sets. Nitric acid was represented by a 25:75 mixture of $HNO_3$ and $H_3O^+$ $NO_3^-$ species in water, with the same parameters as in ref.[61] Simulations with polarization (referred to as POL model), as implemented in AMBER10,[55] used the POL3 model for water[62] and the atomic polarizabilities of other solute and solvent atoms listed in Table S2, in conjunction with selected atomic charges on TBP (SET5) and on uranyl nitrate ($UN_{ESP}$), unless otherwise specified.

Uranyl complexes were simulated with weak harmonic constraints on U···$O_{TBP}$, U···$O_{NO3}$ distances and all $O_{UO2}$···U···$O_{NO3}$ angles (at 2.37 and 2.45 Å and 90°, respectively, with force constants of 50 kcal·mol$^{-1}$·Å$^{-2}$ and 50 kcal·mol$^{-1}$·rad$^{-2}$) to avoid dissociation and to retain a bidentate coordination of nitrates in the equatorial plane (as in an analogous solid state structure[63]) during the dynamics. Nonbonded interactions were calculated with a 12 Å atom-based cutoff, correcting for the long-range electrostatics by using the Ewald summation method (PME approximation).[64] The solutions were simulated with 3D-periodic boundary conditions, thus as alternating slabs of water and "oil" in the case of juxtaposed liquids. Their characteristics and labels (**A**–**P**) are given in Table 1.

All systems were first relaxed by 3000 steps of energy minimization and by a MD simulation of 0.5 ns at 300 K and a constant pressure of 1 atm to adjust the densities. Subsequent dynamics were performed at constant volume. The temperature was maintained (unless otherwise specified) at ca. 300 K by coupling the solution to a thermal bath using the Berendsen algorithm[65] with a relaxation time of 0.2 ps. The MD trajectories and velocities were calculated using the Verlet algorithm with a time step of 2 fs, in conjunction with SHAKE constraints on O–H, C–H, and N–H bonds.

**Mixing–Demixing Simulations.** We first equilibrated biphasic solutions at constant pressure ($P$ = 1 atm) to adjust the densities of the two phases, followed by at least 0.1 ns at constant volume. Mixing was then achieved by a MD run of 2 ns at a temperature of 500 K, with Coulombic interactions divided by a factor 1000 to afford "random" distributions. This was followed by demixing simulations with reset electrostatics at 300 K for at least 5 ns (without polarization) or for 3 ns (POL model).

**Analysis of the Trajectories.** The trajectories were saved and analyzed every ps. Solvent and solute densities were calculated as a function of the $z$-coordinate (perpendicular to the interface) in slices of $\Delta z$ = 0.2 Å width, and the position of the "interface" ($z$ = 0; Gibbs dividing surface) was dynamically defined by the intersection of the TBP + hexane and water (or water plus acid, when present) density curves. The densities of solvents and solutes, averaged over the last 1 ns, were plotted as a function of their $z$-position. Interaction energies between the solute and solvent(s) were calculated with a 12 Å cutoff and PME correction. The orientation of phosphoryl groups with respect to the interface was defined by the order parameter $S(z) = \langle(3\cos^2\theta - 1)/2\rangle$, where $\theta$ is the angle between the P═O and $z$ axis (perpendicular to the interface). $S(z)$ was averaged in $\Delta z$ slices of 0.5 Å.

The interface roughness $R$ was defined by the $S_{itf}/xy$ ratio that would be equal to 1 for a perfectly flat interface. The $S_{itf}$ interfacial area was calculated as in ref 66. The diffusion coefficient $D$ of TBP was calculated from the Einstein relation $\langle\Delta r^2\rangle = 6\,D$t, where $r$ defines the position of the center-of-mass of the TBP molecule at time $t$, and averages are calculated over all TBP's in the linear regime, between 1 and 2 ns.

**Potential of Mean Force (PMF) Calculations.** We calculated the Helmholtz free energy profiles $\Delta A(z)$ for interface crossing by selected solutes (TBP, $UO_2(NO_3)_2(TBP)_2$ complex, $UO_2(NO_3)_2$, $UO_2^{2+}$), with either "pH neutral" or acidic water, comparing SET1 to SET5 charges for TBP without polarization (NO-POL models) to keep the study computationally tractable. Additionally, the POL model was tested for TBP and its complex. The position of the solute was defined by the $z$-distance of its center of mass from the interface where $z$ = 0. The solute was gradually moved from the interface (initial state: $\lambda$ = 1) toward the water or the oil phase (final state: $\lambda$ = 0) up to a $z$-distance of 20 Å, by steps $\Delta z$ = 0.5 Å, i.e., $\Delta\lambda$ = 0.025.


dx.doi.org/10.1021/jp411332e | J. Phys. Chem. B 2014, 118, 3133–3149

Table 2. ESP Charges of TBP Obtained with Different Protocoles and Dipole Moment $\mu$ (in D) Calculated in Gas Phase and in the Liquid

| | | | | BLYP/6-311G++(d,p) | | BLYP/6-31G* | |
|---|---|---|---|---|---|---|---|
| | MNDO[a] | Cui (2012)[b] | HF/6-31+G* | this work | ref[c] | this work | ref[c] |
| conformer | NS[d] | NS[d] | $tg^-g$ | $tg^-g$ | $(tgg)^c$ | $tg^-g$ | $(tgg)^c$ |
| atom[e] | **SET1** | **SET2** | **SET3** | **SET4** | **SET5** | **SET6** | **SET7** |
| O | −0.87 | −0.81 | −0.77 | −0.61 | −0.60 | −0.54 | −0.49 |
| P | 1.77 | 1.61 | 1.52 | 1.20 | 1.05 | 0.99 | 0.82 |
| $O_a$ | −0.56 | −0.61 | −0.63 | −0.52 | −0.36 | −0.45 | −0.29 |
| $CH_2$ | 0.24 | 0.30 | 0.37 | 0.27 | 0.12 | 0.26 | 0.11 |
| $CH_2$ | 0.06 | 0.03 | 0.01 | 0.04 | 0.03 | 0.03 | 0.03 |
| $CH_2$ | 0.02 | 0.04 | 0.07 | 0.08 | 0.03 | 0.07 | 0.02 |
| $CH_3$ | 0.02 | −0.03 | −0.07 | −0.05 | 0.03 | −0.04 | 0.02 |
| $\mu$ *ggg* (opt QM gas)[f] | 1.7 | / | 1.1 | 1.1 | 1.1 | 1.0 | 1.0 |
| $\mu$ *ggg* (opt AMBER gas)[g] | 3.1 | 1.5 | 0.7 | 0.9 | 2.8 | | 2.4 |
| $\langle\mu\rangle$ gas (0.1 ns AMBER, initially *tg*-*g*) | 3.1 (1.1) | 2.5 (1.3) | 1.8 (0.9) | 2.1 (1.0) | 3.1 (1.2) | 2.1 (1.0) | 3.0 (0.9) |
| $\langle\mu\rangle_{TBP}$ liquid (1 ns AMBER)[g] | 3.7 (0.1) | 2.5 (0.1) | 2.2 (0.1) | 2.4 (0.1) | 3.5 (0.1) | / | / |

[a]Calculated here using the charges from P. Beudaert et al. *Solvent Extr. Ion Exch.* **1998**, *16*, 597. [b]S. Cui et al. *J. Phys. Chem. B.*, **2012**, *116*, 305. Charges calculated at the HF/6-31+G* level on a BLYP/TZVP optimized structure. [c]R. Schurhammer et al. *J. Phys. Chem. A*, **2005**, *109*, 5208. The charges have been fitted on the *tgg* form of the TMP (trimethylphosphate) analogue of TBP, and adpated for TBP. [d]Conformer not specified. [e]Atom charges, given in the column in the order O═P−O−$CH_2$−$CH_2$−$CH_2$−$CH_3$. [f]Uses the QM method indicated in this column. [g]Uses the AMBER Charges indicated in this column.

$$\Delta A = \int_0^1 \left\langle \frac{\partial U}{\partial \lambda} \right\rangle_\lambda d\lambda \quad (2)$$

The change in free energy at each step $\lambda$ was calculated using the thermodynamic integration method (TI) based on eq 2.[67] At each $\lambda$ step, we performed 0.5 ns of equilibration plus 1.0 ns of data collection and averaging, requiring a total simulated time of 60 ns per PMF. This is about twice larger than that used by Jayasinghe and Beck in a similar PMF study[40] and large enough to allow for significant diffusion and sampling of TBP, water, and acid molecules along the PMF (see below and ref 66). A PMF with longer sampling (0.5 + 2 ns per step) was also calculated. Along the PMF simulation, as the solute is moved away from the interface, the precise *z*-location of the interface may be somewhat shifted. We thus recalculated the crossing of the solvents density curves at every step of the PMF, and used this updated reference for the $\Delta A(z)$ curves presented here.

**QM Calculations.** All structures were optimized at the DFT/B3LYP or HF levels of theory using the Gaussian09 software.[68] The H, C, N, O, P atoms of the ligands and the O atoms of uranyl were described by the 6-31G* or 6-311++G(d,p) basis set.[68] Hereafter, we name the DFT results obtained with these two basis sets QM1 and QM2, respectively. For the U atom we used the small-core relativistic effective core potential (ECP) of the Stuttgart−Dresden group (SDD) together with their valence basis sets from which each most diffuse s-, p-, d-, and f-function was omitted, affording a [7s6p5d3f] contraction.[69]

## RESULTS

**1. About the TBP "Polarity" Obtained with Different Charge Sets: Force Field vs QM Results in the Gas Phase and TBP Solvation Properties.** Before presenting the PMF and MD results on biphasic systems (Sections 2−4), it is worth first discussing how the choice of TBP charges impacts the TBP "polarity" and its interactions with relevant species of the extraction process. We also explore their effect on the solvation free energies of free and complexed TBP, as well as on the properties of pure liquid TBP and of its aqueous interface.

*TBP Polarity and TBP Conformation in the Gas Phase.* We considered SET1 to SET7 charge sets, labeled by decreasing $P^{\delta+}$═$O^{\delta-}$ polarity, with $q_P$ ranging from 1.77 to 0.99 e and $q_O$ from −0.87 to −0.54 e (see Table 2). Four SETs come from the literature (SET1 with MNDO charges,[34] SET2 from Cui et al.,[42] SET5 and SET7 from Schurhammer et al.[43] have been fitted on the TMP analogue of TBP), whereas SET3, SET4, and SET6 have been obtained in this work. Note that the same QM level may afford different charges when fitted on different TBP conformers. For instance, when the O═P−O−C dihedrals turn from *tgg* to $gg^-g$, $q_P$ increases from 0.87 to 1.04 e (BLYP/6-31G* calculations; see Table S3). Furthermore, the polarity orders of the $P^{\delta+}$═$O^{\delta-}$ and $O^{\delta-}$−$C^{\delta+}$ bonds are not always the same: the latter become more polar from SET1 to SET3, but generally less polar from SET5 to SET7. As a result, the dipole moment $\mu$(TBP) of a given optimized conformer does not regularly decrease from SET1 to SET7 (see, for example, the $tg^-g$ form in Table 2). The same feature is found for the average dipole moments $\langle\mu\rangle_{gas}$ in the gas phase (Table S3). There is thus no clear-cut classification of the TBP "polarity" in this series. Both P═O bond polarity and molecular dipole moment $\mu$(TBP) indicate that SET1 is the most polar model, while SET7 is the least polar. This is consistent with the calculated H-bond energies with $H_2O$ and $HNO_3$ and with the complexation energies of TBP with uranyl nitrate, as well as with the hydration free energies of TBP (see below).

Comparing now different conformers, one sees that $\mu$(TBP) is lowest for the *ggg* form (from 1.3 to 2.8 D, depending on the charges) and highest for the *ttt* and *ttg* forms with the different SETs, as observed by QM1 or QM2 calculations (Table S3). The different studied SETs (SET1, SET2, SET4, SET5, and SET7), like QM1 or QM2 approaches, predict the *ggg* form (of $C_3$ symmetry, assuming all-*trans* butyl chains) to be the most stable one, and that the TBP stability decreases when the O-butyl groups turn from *g* to *t*. In particular, the *ttt* and *ttg* forms are of highest energy. Thus, in the gas phase or in weakly polar media, TBP mainly exchanges between *ggg* and $gg^-g$ forms (and their symmetry equivalents) that contribute to its average


dx.doi.org/10.1021/jp411332e | J. Phys. Chem. B 2014, 118, 3133−3149

dipole moment, with possible modulations in solution (see, for instance, ref 34 for MD results with SET1, and Table S3 for QM1 and QM2 results in PCM−water).

*TBP Interactions with Polar Species in the Gas Phase.* The interaction energies $\Delta E$ between TBP (SET1 to SET7 models) and $H_2O$, $HNO_3$ or $UO_2(NO_3)_2$ are reported in Tables S4 and S5, and compared to QM values obtained with the TMP (trimethylphosphate) analogue of TBP. Interactions with $H_2O$ and $HNO_3$ (reference QM values are $\Delta E$ = −7.0 and −12.2 kcal/mol, respectively) decrease from SET1 to SET7, i.e., with the $q_O$ charge. They are clearly exaggerated with SET1 to SET3 charges, while SET4 to SET7 yield better agreement, especially with respect to $H_2O$ (TIP3P). Adding polarization in the force field has little effect on $H_2O$ and $HNO_3$ adducts (<1 kcal/mol).

To test the TBP interactions with uranyl nitrate, we considered either the complexation of $UO_2(NO_3)_2$ by two TBP's or the $H_2O$ displacement by TBP from $UO_2(NO_3)_2(H_2O)_2$ affording the extractable $UO_2(NO_3)_2(TBP)_2$ complex (see Table S5). The corresponding QM energies are $\Delta E_1$ = −49.6 and $\Delta E_2$ = −9.3 kcal/mol, respectively. The AMBER energies have been calculated with SET1, SET3 to SET5, and SET7 TBP models. They depend on the representation of $UO_2(NO_3)_2$ and are, as expected, more attractive (by about 20 kcal/mol) with the $UN_{integer}$ than with the $UN_{ESP}$ charges. With both UN models, however, SET1 and SET3 charges on TBP exaggerate $\Delta E_1$ and $\Delta E_2$, whereas SET7 underestimates these energies. Overall, the best agreement is found with the SET4- or SET5-TBP, in conjunction with $UN_{ESP}$ charges on UN ($\Delta E_1$ = −49.8 or −50.3 kcal/mol, respectively; $\Delta E_2$ = −10.2 or −10.7 kcal/mol, respectively). Adding polarization to these models has little effect (<2 kcal/mol) on $\Delta E_1$ and $\Delta E_2$.

*The Effect of Charges Distributions on Free Energies of Solvation of TBP and Its $UO_2(NO_3)_2(TBP)_2$ Complex in Pure Water, in the Oil Phase, and at the Interface.* We now analyze the impact of charge distribution on the solvation free energies of TBP, of $UO_2(NO_3)_2$ and of their $UO_2(NO_3)_2(TBP)_2$ complex in three solution environments involved in extraction systems: (i) in bulk (TIP3P) water, (ii) in the liquid TBP (simulated with SET1 charges), or (iii) at the water/hexane interface. This is achieved via free energy perturbation calculations,[67] mutating one state to the other, namely, the most polar TBP model (SET1) to the least polar one (SET7) or to SET5 of intermediate polarity, and/or the $UN_{integer}$ to the $UN_{ESP}$ charges of $UO_2(NO_3)_2$. The resulting $\Delta A$ free energies are reported in Table 3. They are noted $\Delta A_{1/7}$ for the SET1 to SET7 mutation on TBP, and $\Delta A_{Integer/ESP}$ for the mutation on uranyl nitrate.

Mutating the charges of a single TBP molecule has a marked effect in water: $\Delta A_{1/7}$ = 8.6 kcal/mol, and $\Delta A_{1/5}$ = 5.8 kcal/mol from SET1 to SET5. In the neat TBP liquid, $\Delta A_{1/7}$ is smaller than in water, as expected (1.3 kcal/mol). At the interface, however, $\Delta A_{1/7}$ and $\Delta A_{1/5}$ (6.9 and 4.8 kcal/mol, respectively) are closer to the $\Delta A$'s obtained in pure water, in keeping with the solvation of the polar moiety of TBP by interfacial water.

Regarding the water-soluble $UO_2(NO_3)_2$ species (associated salt), the hydration free energy is much more negative with the $UN_{integer}$ than with the $UN_{ESP}$ model, by $\Delta A_{Integer/ESP}$ = 49.5 kcal/mol. Thus, the free energy of transfer of $UO_2(NO_3)_2$ from water to the "oil" phase will be higher with the $UN_{integer}$ than with the more "realistic" $UN_{ESP}$ model (see below).

Similar tests were performed for the $UO_2(NO_3)_2(TBP)_2$ complex, mutating separately the TBP and the $UO_2(NO_3)_2$ charges (see Table 3). In water, the latter mutation yields a much higher energy ($\Delta A_{integer/ESP}$ = 21.7 kcal/mol) than mutating the TBP charges from SET1 to SET7 (3.4 kcal/mol) or to SET5 (1.9 kcal/mol). In pure liquid TBP, the corresponding $\Delta A$'s are smaller, or even negative: $\Delta A_{integer/ESP}$ = 6.1 kcal/mol and $\Delta A_{1/7}$ = −0.3 kcal/mol. At the interface, $\Delta A_{integer/ESP}$ is again higher than $\Delta A_{1/7}$ = (11.2 and 1.1 kcal/mol, respectively), demonstrating the critical role of ions representation on the affinity of their complex for the interface, and thus on its free energy of transfer from water to oil. Conversely, the precise positioning of the uranyl salt (free or complexed) with respect to interfacial water should be modulated by electronic reorganization effects, as modeled by the above mutations.

**Table 3. Difference in Free Energies of Solvation as a Function of the Charge Model of TBP and of Uranyl Nitrate (UN)**

| solute−solvent | initial charges UN/SET | final charges UN/SET | $\Delta A$ (kcal/mol) |
|---|---|---|---|
| 1 TBP in water | SET7 | SET1 | −8.6 |
| | SET5 | SET1 | −5.8 |
| | SET3 | SET1 | −0.9 |
| 1 TBP in liquid TBP[a] | SET7 | SET1 | −1.3 |
| 1 TBP at the interface[b] | SET7 | SET1 | −6.9 |
| | SET5 | SET1 | −4.8 |
| $UO_2(NO_3)_2$ in water | $UN_{integer}$ | $UN_{ESP}$ | 49.5 |
| | | $UN_{Kerisit}$[c] | −20.0 |
| $UO_2(NO_3)_2(TBP)_2$ in water | $UN_{integer}$/SET1 | $UN_{ESP}$/SET1 | 21.7 |
| | | $UN_{Kerisit}$[c]/SET1 | 3.4 |
| | | UN "all ESP" | 19.4 |
| | | $UN_{integer}$/SET7 | 3.4 |
| | | $UN_{integer}$/SET5 | 1.9 |
| $UO_2(NO_3)_2(TBP)_2$ in pure liquid TBP[a] | $UN_{integer}$/SET1 | $UN_{ESP}$/SET1 | 6.1 |
| | | $UN_{integer}$/SET5 | −0.3 |
| $UO_2(NO_3)_2(TBP)_2$ at the interface[b] | $UN_{integer}$/SET1 | $UN_{ESP}$/SET1 | 11.2 |
| | | $UN_{integer}$/SET5 | 1.1 |

[a]Liquid TBP simulated with SET1 charges. [b]Hexane/water (TIP3P) interface. [c]Uranyl charges: $q_U$ = +3.50 and $q_O$ = −0.75 e. Kerisit, S. and Liu, C. *J. Phys. Chem. A* **2013**, *117*, 6421.

*TBP Polarity and Properties of the Pure Liquid.* Because the calculated properties of liquid TBP can be affected by the force field parameters,[42] we decided to compare the SET1 to SET5 and POL models. The results (see Figures 1 and S1) indeed confirm the effect of charges distribution on the structure of the liquid,[42] as judged from the P···P, P···O, and O···O RDFs that display a broad peak in the 4−5 Å domain with the SET2 to SET4 charges, but not with SET1 or SET5. There is thus no regular evolution of the RDFs as a function of the P═O bond polarity, i.e., from SET1 to SET5.

Regarding the electric properties, one first observes that the average dipole moment $\langle\mu\rangle_{TBP}$ in the liquid is comparable, with a given charge SET, to $\langle\mu\rangle_{gas}$ in the gas phase, because TBP adopts similar conformations in both phases (see, for instance, the statistics of O═P−O−C dihedrals that are mainly *gauche*; see Figure S2). Modulations of $\langle\mu\rangle_{TBP}$ are thus mainly caused by the choice of charges. Comparing now different charge SETs, one can see that $\langle\mu\rangle_{TBP}$ is lower with SET2 to SET4 (2.2 to 2.5 D) than with SET1 and SET5 (3.7 and 3.5 ± 0.1 D, respectively), which suggests that the lack of "first peak" in the RDFs with SET1 and SET5 likely corresponds to lessened interactions between polar moieties within the liquid. This


dx.doi.org/10.1021/jp411332e | J. Phys. Chem. B 2014, 118, 3133−3149

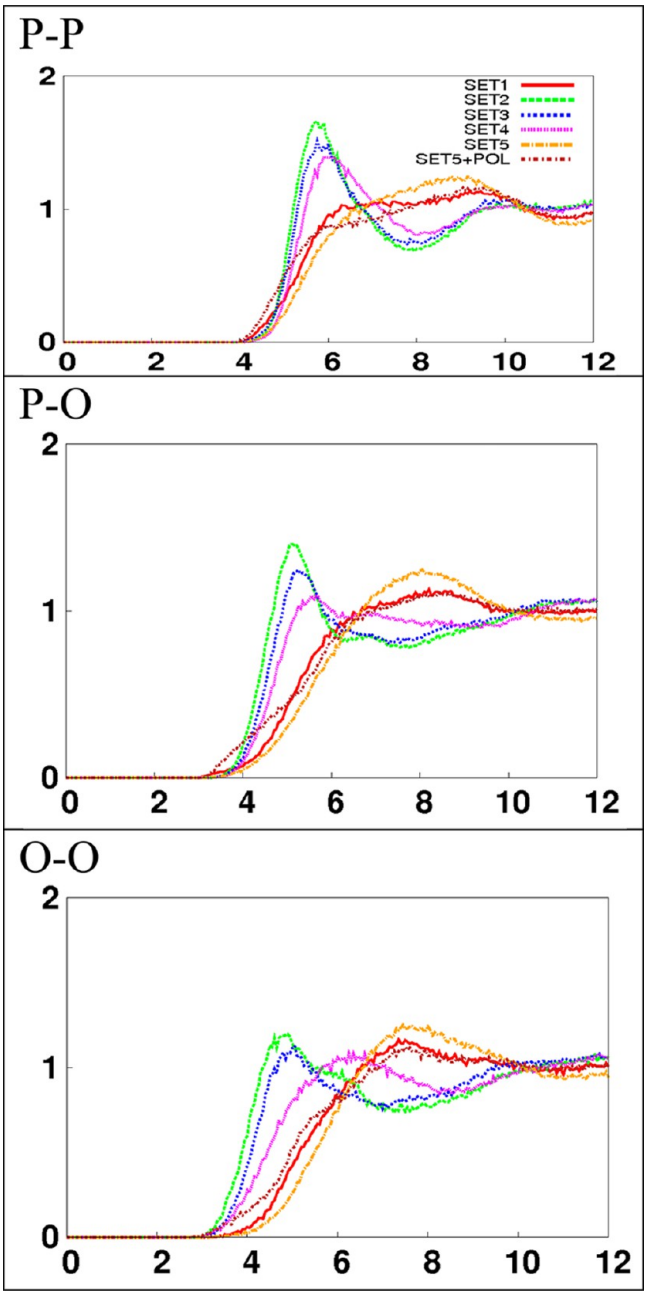


**Figure 1.** Pure liquid TBP (system **A**): RDFs P···P, P···O, and O···O (O = phosphoryl oxygen), obtained with different TBP models (red: SET1; green: SET2; blue: SET3; pink: SET4; orange: SET5; brown: SET5+POL).

feature seems to be consistent with the evolution of diffusion coefficients $D$ that are somewhat higher and closer to the experimental value of 0.023 Å$^2$/ps[70] with SET1 and SET5 ($D \approx$ 0.017 Å$^2$/ps), than with SET2 to SET4 ($D$ = 0.010, 0.005, and 0.015 Å$^2$/ps, respectively). Comparing now the SET5 (NO-POL) to POL results shows that the different RDFs are similar, but diffusion is higher with polarization ($D \approx$ 0.031 Å$^2$/ps).

Further insights into the effect of TBP charges come from the analysis of "cohesive forces" of the liquid, simulated with SET1 to SET5 models. For this purpose, we calculated the average interaction energy $\langle \Delta E \rangle$ of each TBP with all others of the liquid, as well as the corresponding van der Waals and electrostatic contributions: $\langle \Delta E \rangle = \langle \Delta E_{vdw} \rangle + \langle \Delta E_{elec} \rangle$. The results (Figure S1) indicate that $\langle \Delta E_{vdw} \rangle$ is fairly constant ($\approx -44 \pm 0.5$ kcal/mol) with the different charge SETs and higher in magnitude than $\langle \Delta E_{elec} \rangle$ (from −3.3 to −6.1 ± 0.5 kcal/mol, depending on the TBP charges). Interestingly, $\langle \Delta E \rangle$ is somewhat less attractive (by ≈3 kcal/mol) with SET1, SET4, or SET5 than with SET2 or SET3, supporting the view that the variants in the studied RDFs relate to subtle modulations of Coulombic TBP···TBP interactions.

Comparing now the calculated dipole moment $\langle \mu \rangle_{TBP}$ in the liquid to the experimental value of 3.1−3.2 D in organic solvents,[71,72] one sees that it is somewhat overestimated with SET1 (3.7 D) and underestimated with SET2, SET3, and SET4 (2.5, 2.2, and 2.4 ± 0.1 D, respectively), while SET5 performs best in the series (3.5 D).

*The Pure-TBP/Water Interface, Simulated with Different Models.* The biphasic pure-TBP/water solution was simulated for at least 5 ns with either SET1, SET5, or SET7 charges on TBP, as well as with the POL model. As seen from final snapshots and density curves (Figures 2, S3 and S4), the overall picture of the interface and intersolvent mixing features look similar with the SET5, SET7 or POL models, i.e., without local intersolvent mixing (Figure S4). In these cases, the interface roughness ($R$ = 1.88, 1.64, and 1.93 ± 0.10, respectively) is mainly caused by fluctuations of the oil and water surfaces, and the solvent densities reach their bulk values at about 8−10 Å from the Gibbs surface. With the SET1 model, the "interface" is

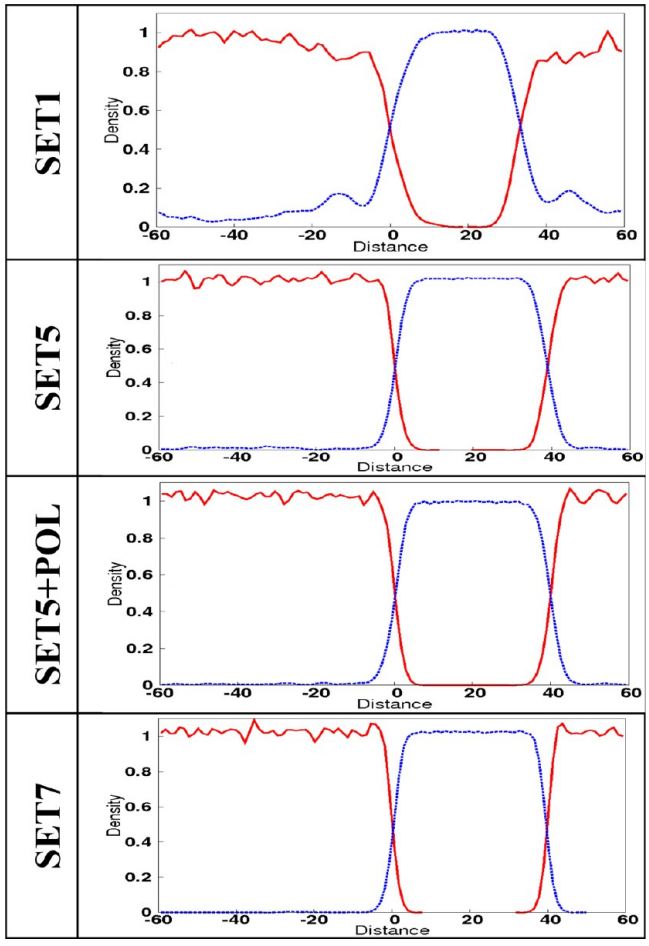


**Figure 2.** Pure TBP/water interface (system **B**): density curves of TBP (red) and water (blue). Snapshots of the liquids are given in Figure S3.


dx.doi.org/10.1021/jp411332e | J. Phys. Chem. B 2014, 118, 3133−3149

much broader, ill-defined, more rough ($R > 2.8 \pm 0.4$), and involves a mixture of TBP and $H_2O$ molecules, extending beyond 15 Å from the interface, according to the water density on the oil side. Furthermore, the amount of "extracted" water has not reached a plateau after 5 or 10 ns (Figure S14), in keeping with the exaggerated humidity of the bulk TBP phase with the SET1 model (see Discussion section).

At this stage, there is thus no firm criteria to select "the best" model. However, in many respects, the SET5 used in the following without polarization (NO-POL calculations) or with added polarization on all atoms (POL calculations) appears as a valuable alternative over the most polar one (SET1) used so far. Further comparisons involving biphasic systems are presented below.

**2. The "Neat" TBP + Hexane/Water Interface with "Neutral" versus Acidic Water.** We now turn to the neat TBP+hexane/water interface (without uranyl nitrate), simulated for 5 ns with the SET1, SET5, and SET7 charges (NO-POL), and with the POL model (SET5+POL), in either pH-neutral or acidic conditions. As seen from the final snapshots and density curves (Figures 3, S5 and S8), TBP is diluted in the hexane phase but accumulates at the two interfaces. In the different cases, the order factor $S$ of P═O bonds, zero on the average in the bulk oil phase, peaks at $S \approx 0.2$ near the interface, indicating some ordering with a tilt angle of ≈45°, on the average. As a result, the average $\langle \mu_z \rangle$-component of the TBP dipole moment amounts to ≈2.0 D at the interface.

In no case is the interface fully covered by TBPs (see Figures 4, S6, and S9). Within 10 Å from the interface, one finds about 26, 26, 18, and 19 ± 1 TBP's, respectively, with the SET1, SET5, SET7, and POL models in pH neutral conditions. When water gets acidified, these numbers (normalized to a same *xy* section area) are comparable (23, 22, 19, and 21 ± 1 TBPs, respectively), yielding an interfacial area of ≈70 to 85 Å$^2$, on the average per TBP. Similar values are obtained at higher TBP concentration (1.5 M, see also Figures S11 and S13), which suggests that the interface unsaturation stems neither from an insufficient TBP concentration nor from too weak attractions by interfacial water (see, for instance, the energy component analysis in Table S6), but from the dominant *gauche* over *trans* forms of TBP. The latter would be more amphiphilic, but are less stable. As a result, most interfacial TBPs of the 1.1 M solution (≈50% during 1 ns and ≈80% during 4 ns) exchange with the bulk oil phase (see cumulated trajectories of selected TBP's in Figures 5, S7, and S10, and histograms of lifetimes at the interface in Figure S16), at higher rate with the SET7 than with SET5 or SET1 charges, i.e., when TBP gets less attracted by interfacial water. Regarding the effect of polarization (POL versus SET5 trajectories) two main features appear: the number of TBPs at the interface decreases (by ≈4 TBPs), whereas the number of exchanges increase (by ≈3 TBPs) during the dynamics. These results are consistent with the reduced dipole moment of POL3 water at the interface compared to that in bulk water (2.2 and 2.6 D, respectively at the water/$CCl_4$ interface)[25,46] or to TIP3P water (2.35 D), thereby lessening the TBP attraction by interfacial water. As expected, exchanges increase with the TBP concentration and with time. For instance, for the 1.5 M TBP solution (SET5 model), 96% of interfacial TBPs exchange during 5 ns with the bulk oil phase (Figure S16), illustrating the high dynamics at the interface.

As for the pure-TBP/water system, the roughness of the TBP +hexane/water interface increases with the TBP polarity, in the order SET7 < SET5 ≈ POL < SET1: $R$ = 1.65, 1.77, 1.78, and 2.25 ± 0.23, respectively, for the pH neutral system and $R$ = 1.80, 2.04, 2.18, and 2.55 ± 0.27, respectively for the acidic systems. At the interface, each (P)O phosphoryl oxygen is mainly H-bonded to $H_2O$ protons at neutral pH (2.0, 1.5, and 1.5 water protons within 2.6 Å, respectively, with the SET1, SET5, and POL models). This is somewhat less than in pure water (2.3, 2.0, and 2.0 $H_2O$ protons, respectively). In acidic conditions, (P)O binds 0.7, 1.4, and 1.4 $H_2O$ protons, respectively, and little $HNO_3$ (0.2 molecules with the three models). TBP···$H_3O^+$ contacts are observed only with the SET1 charges (0.8 protons per TBP) that better account the corresponding interaction energy than do the SET5 or POL models, when compared to QM value (−53 kcal/mol; see Table S4). Furthermore, protonation of TBP by $H_3O^+$ cannot be precluded, according to QM results in the gas phase. Thus, no firm conclusion can be drawn regarding acid complexation by TBP at the interface.

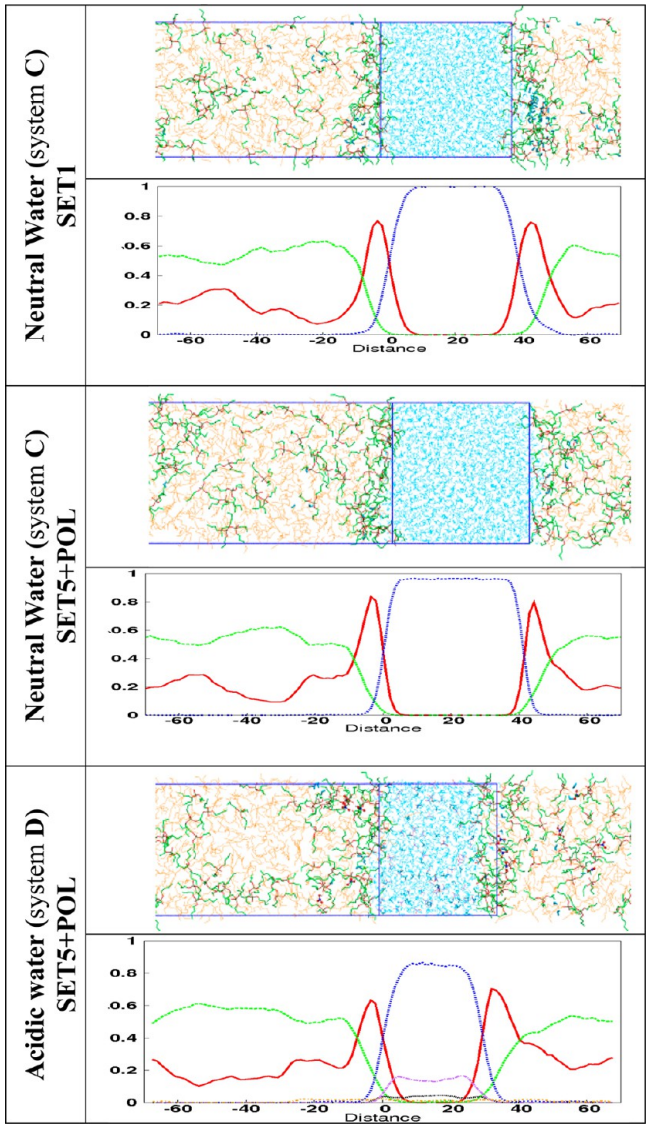


**Figure 3.** Neat $TBP_{1.1M}$ + hexane/water interface. For each system, top: snapshot after 2−5 ns of dynamics, bottom: density curves (TBP: red; hexane: green; water: blue; $HNO_3$: orange; $H_3O^+$: black; $NO_3^-$: purple). See Figures S5 and S8 for the other models, including order factors and dipole moments of TBP.


dx.doi.org/10.1021/jp411332e | J. Phys. Chem. B 2014, 118, 3133−3149

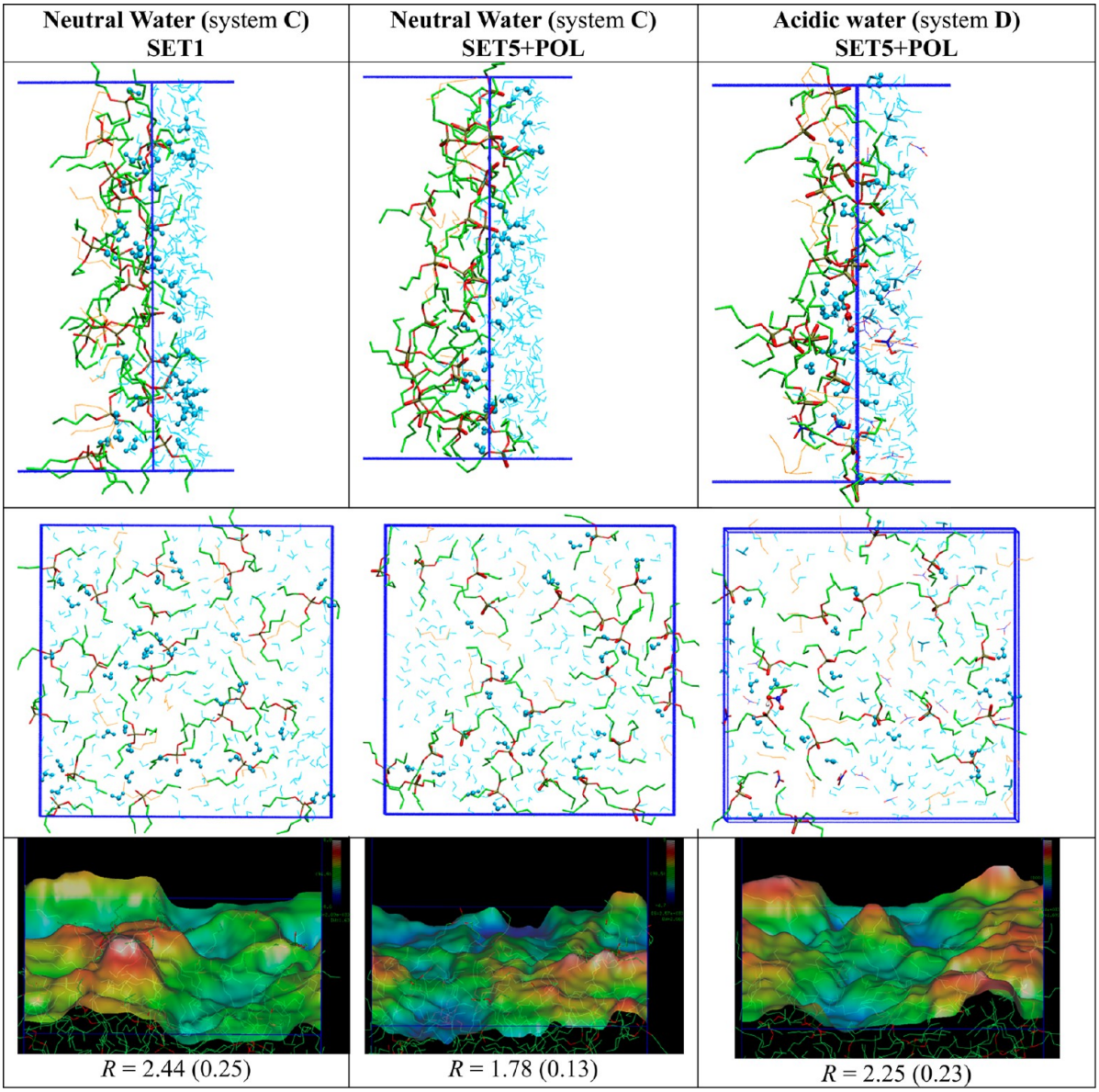


**Figure 4.** Neat $TBP_{1.1M}$ + hexane/water interface. Side view, *xy* view (highlighting P═O···$H_2O$ interactions) and interfacial surface. See Figures S6 and S9 for the other models.

**3. Free Energy Profiles for Interface Crossing by TBP and Its Uranyl Nitrate Complex.** The free energy profiles $\Delta A(z)$ for transferring a single TBP molecule or its neutral $UO_2(NO_3)_2(TBP)_2$ complex across the hexane/neutral water interface are shown in Figures 6−8. A common feature of these hydrophobic species concerns their partitioning between the two phases: with the different models, the $\Delta A_{WO}$ free energy difference is negative, correctly predicting that TBP and its complex prefer the oil phase. Furthermore, in many cases, $\Delta A(z)$ displays a minimum on the oil side of the interface (I position, at $z \approx -5$ Å).

*Transfer of a Single TBP Molecule.* Since the precise charge distribution can drastically affect the partitioning and surface activity of neutral molecules,[73] we decided to first simulate the transfer of a single TBP across the "neat" hexane/water interface (without other TBPs), comparing SET5 to SET1 and SET7 models. As expected, the preference for the oil phase decreases when TBP gets more polar (and thus more attracted by water), in the order SET1 < SET5 < SET7 ($\Delta A_{WO}$ = −3.8, −8.6 and −9.4 kcal/mol, respectively). With the three models, $\Delta A(z)$ displays a minimum near the interface, that decreases in depth from SET1 to SET7 ($\Delta A_{IO}$ = 8.2, 4.5, and 3.0 kcal/mol, respectively). Indeed, at the interface, the phosphate head is well solvated by water, whereas the butyl chains are mostly solvated by hexane (see Figure 6). With SET5 or SET7 charges, the TBP is equally attracted by water and hexane at the interface (by ≈20 kcal/mol), while with the SET1 charges, it is more attracted by water (by ≈10 kcal/mol; see Table S7). Taking into account polarization effects does not significantly change the free energy profiles, if one compares the POL to the SET5 (NO-POL) results: with polarization, the TBP molecule becomes somewhat less hydrophobic ($\Delta A_{WO}$ = −7.2 versus −8.6 kcal/mol). It also becomes less surface active ($\Delta A_{IO}$ = 2.6 versus 4.5 kcal/mol), in keeping with its lower attractions by POL3 than by TIP3P water at the interface (their permanent dipole moments are 1.98 and 2.25 D, respectively). This feature is fully consistent with the higher rate of TBP exchanges


dx.doi.org/10.1021/jp411332e | J. Phys. Chem. B 2014, 118, 3133−3149

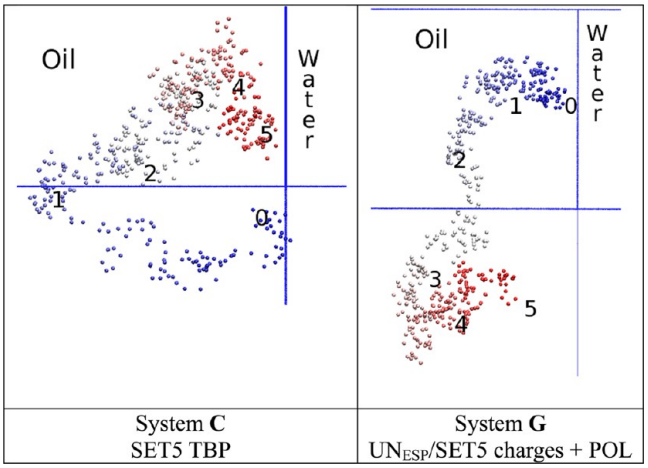


**Figure 5.** Trajectory of the center of mass of a TBP molecule (left) and of a $UO_2(NO_3)_2(TBP)_2$ complex (right) at the neat TBP + hexane/water interface, labeled and colored from blue (0 ns) to red (5 ns) as a function of time. The interface ($z$ = 0) is marked with a vertical blue line.

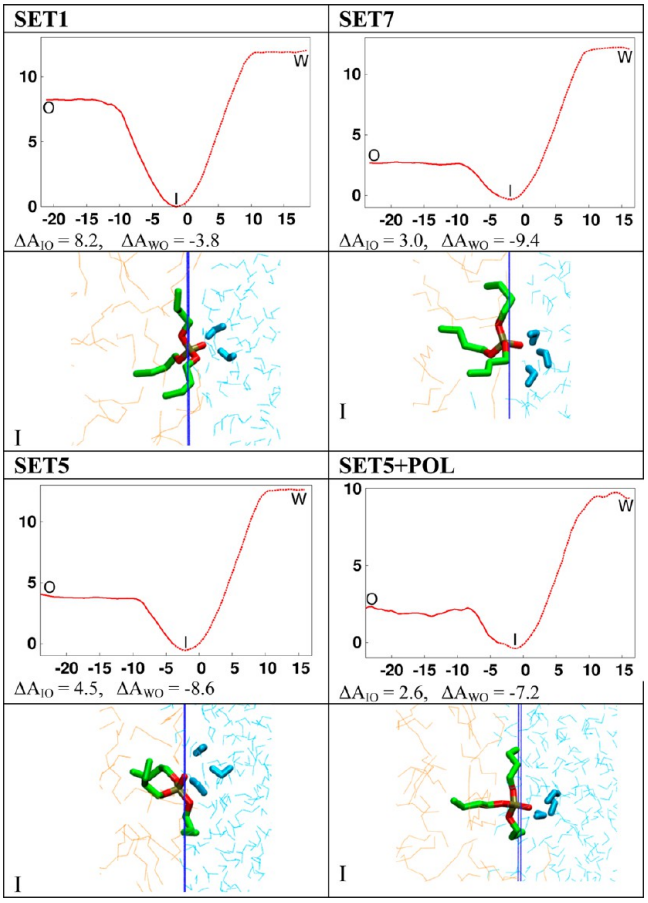


**Figure 6.** Interface crossing by 1 TBP, from hexane to neutral water (system **H**): free energy profile (Δ$A$ in kcal/mol) and snapshots at the interface (I position). Snapshots at the O and W positions are given in Figure S17.

between the interface and the oil phase reported above with the POL, compared to the SET5 (NO-POL) model.

To investigate the effect of TBP concentration on interface crossing, we considered the 1.1 M TBP solution in hexane, comparing the two "extreme" SET1 and SET7 models for all TBPs of the solution. With both models, the $\Delta A_{WO}$ energy difference becomes somewhat higher than at "infinite" TBP dilution (by $\Delta\Delta A_{WO}$ = 1.6 and 1.9 kcal/mol, respectively; see Figure 7), in keeping with the improved solvation of TBP by other TBPs in the oil phase (see for instance snapshots in Figure S18). Furthermore, the interfacial activity of TBP becomes now negligible ($\Delta A_{IO}$ = 0.0 kcal/mol with SET1 and −1.0 kcal/mol with SET7), since the TBP leaving the interface can be replaced by another TBP from bulk phase, as observed along the unconstrained dynamics with the SET1, SET5, or POL model.

*Transfer of a $UO_2(NO_3)_2(TBP)_2$ Complex.* For the $UO_2(NO_3)_2(TBP)_2$ neutral complex, four PMFs were first simulated with the 1.1 M TBP solution, combining two TBP models (SET1 versus SET5 on all TBP's) with two UN models ($UN_{integer}$ versus $UN_{ESP}$). They reveal a clear model dependence, especially for uranyl nitrate (see Figures 8 and S19). In fact, with $UN_{integer}$ charges, the free energy profile $\Delta A(z)$ displays a minimum near $z \approx -5$ Å, that is deeper with SET5 than with SET1 ($\Delta A_{IO}$ = 5.8 and 3.8 kcal/mol, respectively). We note that this trend is opposite to the one observed for TBP itself, because the phosphate group of TBP ligands has no contact with water. Furthermore, the SET1−TBP complex is less hydrophobic than the SET5−TBP one ($\Delta A_{IW} \approx$ 13 and 16 kcal/mol, respectively) and is better solvated in the oil phase by other SET1−TBPs and dragged water.

The most dramatic changes are observed with the $UN_{ESP}$ charges on uranyl nitrate, combined with either SET1− or SET5−TBPs: now $\Delta A(z)$ regularly decreases from the aqueous to the oil phase, without displaying any peculiar feature near the interface, indicating that the $UO_2(NO_3)_2(TBP)_2$ complex is no more surface active. This feature mainly stems from the reduced hydration of the complex in the aqueous phase (and, to a lesser extent, at the interface), as shown by the mutation reactions reported above. As a result, the $\Delta A_{OW}$ energy difference obtained with a given TBP model is ≈14 kcal/mol higher with the $UN_{ESP}$ than with the $UN_{integer}$ charges. See also an energy component analysis in Table S8. Thus, when electronic reorganization effects of complexed uranyl nitrate, as mimicked by the ESP charges, are taken into account, the complex becomes more hydrophobic and can diffuse from the interface to the oil phase without overpassing energy barriers.

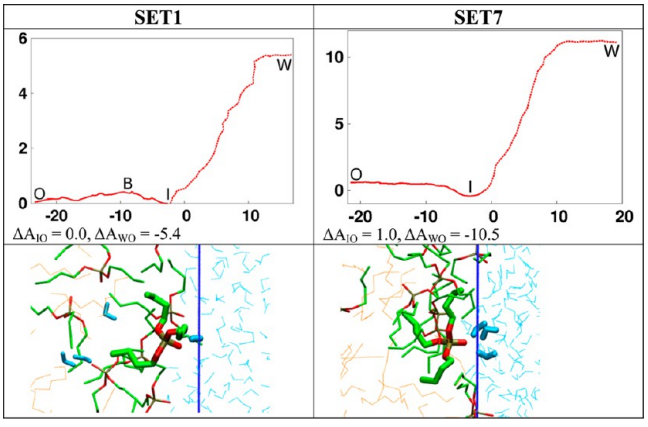


**Figure 7.** Interface crossing by 1 TBP, from $TBP_{1.1M}$ + hexane to neutral water (system **I**): free energy profile (Δ$A$ in kcal/mol) and snapshots at the interface. Snapshots at the O and W positions are given in Figure S18.


dx.doi.org/10.1021/jp411332e | J. Phys. Chem. B 2014, 118, 3133−3149

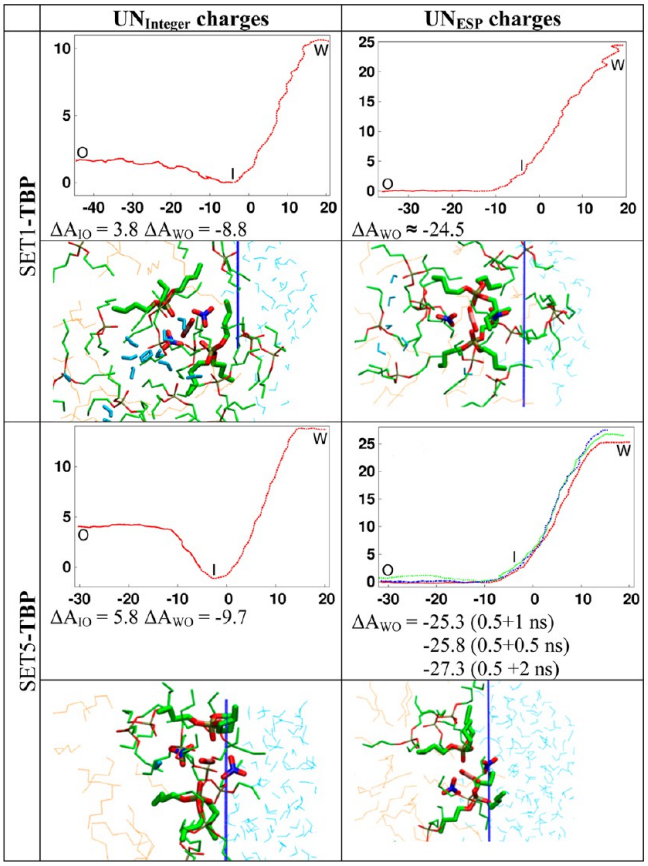


**Figure 8.** Interface crossing by the $UO_2(NO_3)_2(TBP)_2$ complex, from $TBP_{1.1M}$ + hexane to neutral water (system **J**): free energy profiles (ΔA in kcal/mol) and snapshots at the interface (I position). ΔA is calculated with 0.5 + 1 ns (red curve), 0.5 + 0.5 ns (green curve) or 0.5 + 2 ns (blue curve) at each step. Snapshots at the O and W positions are given in Figure S19. See Table S8 for an energy component analysis at the different positions.

Given the importance of the studied complex, we decided to recalculate its PMF (SET5 charges on TBP), with four variants: (i) using different sampling times at each step, namely, a shorter one (0.5 + 0.5 ns) and a longer one (0.5 + 2 ns) instead of the 0.5 + 1 ns used so far. The resulting free energy curves (Figure 8) are quite similar, without mimimum on the oil side of the interface and with $\Delta A_{WO} \approx -25.8$, −27.3, and −25.3 kcal/mol, respectively. (ii) The second variant uses "all-ESP" charges on $UO_2(NO_3)_2(TBP)_2$, obtained from a DFT/B3LYP/6-31G(d,p) calculation on the whole complex, yielding $q_{UO2}$, $q_{NO3}$, and $q_{TBP}$ charges of 0.698, −0.522, and 0.173 e, respectively (Table S1). As shown in Figure 9, the resulting transfer from neutral water to the oil phase is again an energetically downhill process (without barrier near the interface) and the $\Delta A_{WO}$ energy difference (≈ −25 kcal/mol) is close to the one obtained with the $UN_{ESP}$ model. This feature is in keeping with the fact that both models yield similar free energies of solvation in water ($\Delta\Delta A$ = 2.3 kcal/mol; see Table 3), indicating that the change in solvation properties related to electron reorganization within the complex are mainly due to the anion···cation interactions. The third variant (iii) uses the POL model in conjunction with the $UN_{ESP}$ charges on uranyl nitrate. Again, $\Delta A(z)$ decreases from the aqueous to the oil side without displaying a well-defined minimum near the interface (see Figure 9). The main difference between the POL and NO-POL result is the reduced $\Delta A_{WO}$ energy difference between the bulk phases (from ≈25 to 14 kcal/mol). This diminution likely reflects the reduced hydrophobicity of $UO_2(NO_3)_2(TBP)_2$ with the POL model, due to the lower polarity of POL3 water, compared to TIP3P water, at the apolar surface of the complex.

The fourth variant (iv) deals with the effect of added nitric acid (3 M initially in the aqueous phase) on the interface crossing by the $UO_2(NO_3)_2(TBP)_2$ complex, calculated with the NO-POL model and $UN_{ESP}$ charges. The resulting $\Delta A(z)$ curve looks similar to the one obtained using the same charges, but without acid (Figure 9), without minimum near the interface. The main difference concerns the $\Delta A_{OW}$ energy difference that increases from 25 kcal/mol (without acid) to 29

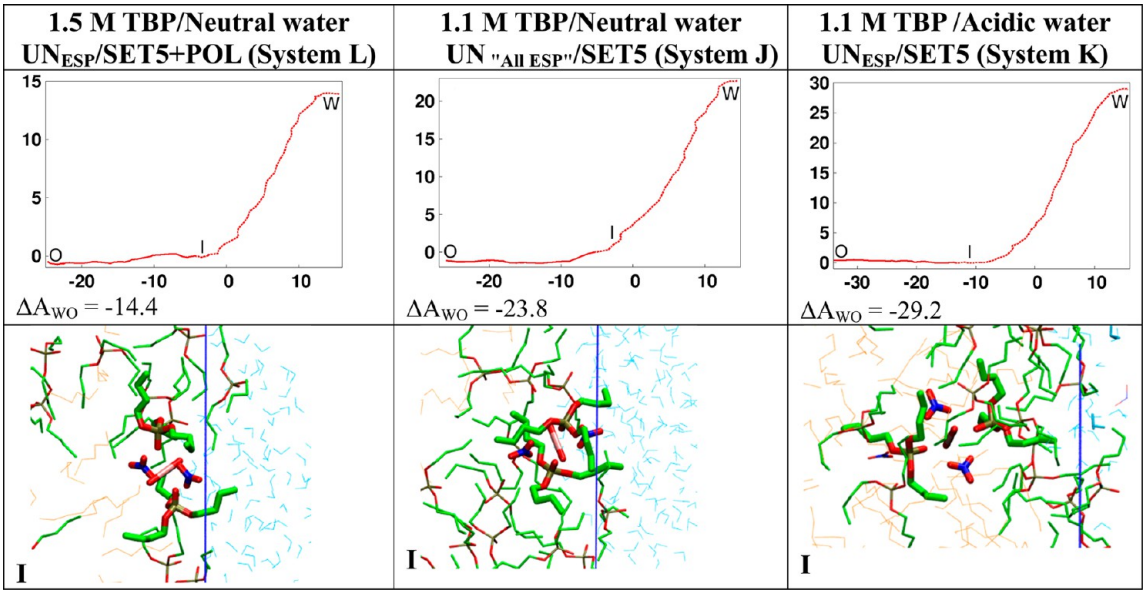


**Figure 9.** Interface crossing by the $UO_2(NO_3)_2(TBP)_2$ complex, from TBP + hexane to neutral or acidic water (systems **J**–**L**): free energy profile ($\Delta A$ in kcal/mol) and snapshots at the interface (I position). Snapshots at the O and W positions are given in Figure S20.


dx.doi.org/10.1021/jp411332e | J. Phys. Chem. B 2014, 118, 3133−3149

kcal/mol (with nitric acid), which is consistent with some salting-out effect of the acid.

**4. Interface Crossing by $UO_2(NO_3)_2$ and $UO_2^{2+}$ Species: Are They Complexed by TBP and Predicted to Be Extracted?** Simulating the transfer of uncomplexed uranyl, either coordinated to its nitrate counterions or "naked", to a TBP-containing phase is quite challenging because it involves two key features of the extraction process: complexation of two TBPs (plus nitrates in the case of the "naked" $UO_2^{2+}$ cation), and transfer to the oil phase. The overall process should be exergonic, i.e., with $\Delta A_{WO}$ negative. The results show that this is indeed the case when $UO_2(NO_3)_2$ is simulated with $UN_{ESP}$, but not with $UN_{integer}$ charges, combined with either SET1 or SET5 TBP models. Likewise, the transfer of the "naked" +2 charged $UO_2^{2+}$ cation to the TBP+hexane phase is calculated to be unfavored, because it is likely too "hydrophilic" and does not spontaneously form the $UO_2(NO_3)_2(TBP)_2$ complex. The PMFs obtained for the two forms of the cation are discussed below.

*Transfer of $UO_2(NO_3)_2$.* When $UO_2(NO_3)_2$ is pulled from the interface to the oil phase, it spontaneously captures two TBPs and forms the $UO_2(NO_3)_2(TBP)_2$ species with the four tested models ($UN_{integer}$/SET5, $UN_{ESP}$/SET5, $UN_{ESP}$/SET1 and $UN_{ESP}$/SET5 charges). This feature is consistent with the higher affinity of $UO_2(NO_3)_2$ for two TBP over two $H_2O$ ligands, as found in QM and AMBER calculations (Table S5). However, the partitioning of the $UO_2(NO_3)_2(TBP)_2$ complex formed along the PMF critically depends on the UN representation (see Figure 10): with $UN_{integer}$ charges, it prefers the aqueous phase, while with $UN_{ESP}$ charges, it prefers the oil phase. Why is this so?

We noted that along these PMFs, the complexes sometimes adopt different *cis*/*trans* stereochemistries in the oil phase, in water or at the interface. To characterize these, we calculated the dipole moment $\mu$ of the $UO_2(NO_3)_2$ "UN" moiety along the PMFs (see Figure S22): typically, $\mu$-*trans* ≈ 1−2 D, while $\mu$-*cis* ≈ 15 D with $UN_{Integer}$ charges or ≈6.5 D with $UN_{ESP}$ charges. *Cis* structures are intrinsically less stable than the *trans* ones, but have higher dipole moments and can be better solvated.[40] For instance, the interaction energies of UN-*cis* and UN-*trans* with TIP3P bulk water are −177 and −145 ± 10 kcal/mol, respectively. Other structures, involving for instance monodentate nitrates, cannot be precluded,[74] but are unexplored here due to the force field limitations and the imposed constraints. With the four models, $UO_2(NO_3)_2$ uncomplexed is found to be *cis* on the water side of the interface, but model-dependent *cis*/*trans* exchanges may occur along the PMFs, indicating that these forms should be close in energy in solution. The preference for the aqueous over the oil phase found with the $UN_{integer}$ model is unlikely to be caused by stereochemical features since this model correctly yields the *trans* $UO_2(NO_3)_2(TBP)_2$ complex in the bulk oil phase (not extracted, however, according to the free energy result). The main explanation can rather be found on the water side, where $UO_2(NO_3)_2$ depicted with $UN_{integer}$ charges is likely too hydrophilic, as suggested by the $UN_{integer}$ to $UN_{ESP}$ charge mutations presented above ($\Delta A$ = 49 kcal/mol). Rising the free energy on the water side of the interface by such an amount would clearly lead to a preference for the oil side, after TBP complexation.

Indeed, the PMFs calculated with $UN_{ESP}$ charges and either SET1- or SET5-TBPs indicate that the extraction of $UO_2(NO_3)_2$ to the oil phase, promoted by the TBPs

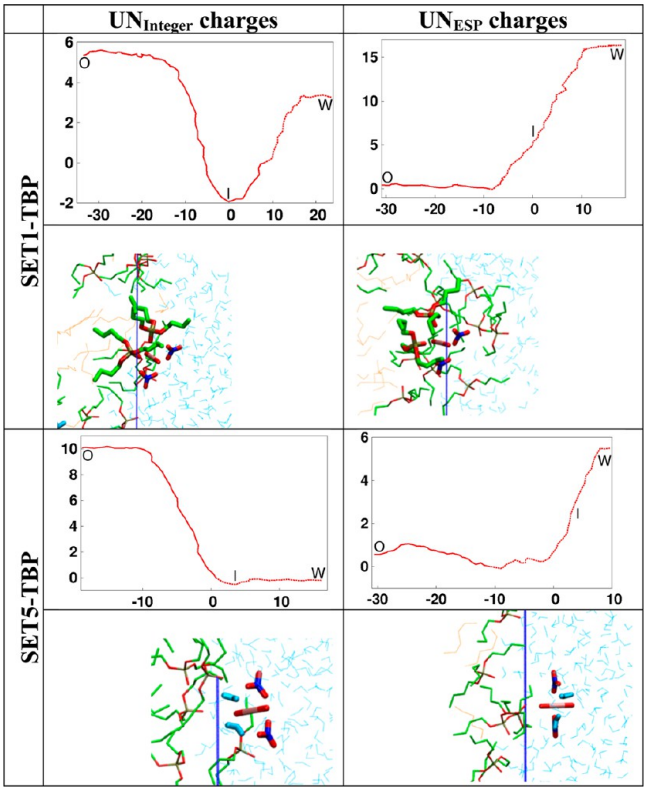


**Figure 10.** Interface crossing by $UO_2(NO_3)_2$, from $TBP_{1.1M}$ + hexane to neutral water (system **M**: free energy profiles ($\Delta A$ in kcal/mol) and snapshots at the interface (position I). Snapshots at the O and W positions are given in Figure S21. See Table S9 for an energy component analysis at the different positions.

complexation, now becomes favored: $\Delta A_{WO}$ ≈ −15 kcal/mol with SET1 and −6 kcal/mol with SET5. The higher $\Delta A_{WO}$ energy found with SET1-TBP includes the higher energy gain upon complexation with $UO_2(NO_3)_2$, as shown by QM and AMBER results (Table S5). With both TBP models, the extracted complex $UO_2(NO_3)_2(TBP)_2$ has now *cis*-ligands and *cis*-nitrates. Further reorganization from *cis* to *trans* would be stabilizing, yielding more negative $\Delta A_{WO}$ energies, thus further favoring extraction. According the to $\Delta A(z)$ curves obtained with $UN_{ESP}$ charges, the complexes formed near the interface should diffuse "freely" to the oil phase, as found above for the preformed $UO_2(NO_3)_2(TBP)_2$ species (simulated with $UN_{ESP}$ charges), i.e., without being adsorbed at the interface.

Figure S23 shows three typical snapshots of $UO_2(NO_3)_2$ near the interface along the PMFs with SET5-TBP and either $UN_{Integer}$ or $UN_{ESP}$ charges (i) just prior to complexation by TBP, (ii) with one TBP complexed, and (iii) its extracted complex with TBP. In all cases, TBP complexation occurs on the oil side of the interface (Z ≈ −6 to −8 Å) where UN is still connected to the bulk water phase by small "water fingers". The overall interface remains rather flat, with a small local "water cone" dragged by the salt, somewhat larger when UN gets more polar, as found previously.[40]

*Transfer of the "naked" $UO_2^{2+}$ cation.* We performed five PMF simulations for the "naked" +2 charged uranyl cation: two with neutral water and two with acidic water, with either SET5 or SET1 TBP model, starting after 1 ns of equibration with $UO_2^{2+}$ near the interface. In a fifth simulation, $UO_2^{2+}$ was placed initially in close contact with TBP and two $NO_3^-$ counterions, as in the $UO_2(NO_3)_2(TBP)_2$ complex, to favor


dx.doi.org/10.1021/jp411332e | J. Phys. Chem. B 2014, 118, 3133−3149

complexation. Pulling uranyl to the oil phase did not afford however, the neutral $UO_2(NO_3)_2(TBP)_2$ neutral species. Futhermore, the changes in free energies from water to oil were not in favor of uranyl extraction, even when the hydrophobic $UO_2(NO_3)_2(TBP)_3$ species was formed (see Figures S24 and S25 and snapshots of the different uranyl species formed at the I, O and W positions along these PMFs).

We note that these PMF results on "naked" uranyl transfer, somewhat disappointing, are consistent with those obtained for $UO_2(NO_3)_2$ depicted with the $UN_{integer}$ model that appears to be too hydrophilic to correctly predict the partitioning of the $UO_2(NO_3)_2(TBP)_2$ complex formed along the PMF. A fortiori, using a more polar +2 charged uranyl model (as recently developed by Kerisit et al., with $q_U$ = +3.50 and $q_O$ = −0.75 e)[76] would render $UO_2(NO_3)_2$ more hydrophilic (by 20 kcal/mol, according to the $UN_{integer}$ to $UN_{Kerisit}$ mutation; see Table 3), further preventing its transfer to the oil phase. Thus, simultaneously accounting for the hydration free energy of "naked" uranyl ion (to develop its nonbonded parameters),[59,76] for its ion-pairing and complexation features, and partitioning between two immiscible liquids remains a challenging issue, requiring further developments, including QM representations of the potential energy.[77,78] The transfer of single neutral entities like TBP or its preformed $UO_2(NO_3)_2(TBP)_2$ complex is less problematic, but still model dependent, as seen from the above model comparisons.

## DISCUSSION AND CONCLUSIONS

We have reported MD and PMF investigations of the interfacial landscape involved in the liquid−liquid extraction of uranyl nitrate by TBP, comparing several models where noncovalent interactions are represented by pairwise additive 1−6−12 potentials. Furthermore, the effect of polarization of solvents and solutes has been tested in conjunction with a reasonable choice of TBP charges. Regarding TBP, it appears that for many purposes, the SET5 set of charges is more balanced than the most polar SET1 one. It better accounts for the TBP interactions with key species ($H_2O$, $HNO_3$ or $UO_2(NO_3)_2$) in the gas phase, or for the dipole moment of TBP in the liquid. Other key aspects are discussed below, focusing on the thermodynamics of TBP at the interface and the "humidity" of the oil phase. We then address the most critical feature in the context of assisted ion extraction, namely the representation of the extracted ions that determines their interfacial behavior in their uncomplexed and complexed states, thereby impacting the uranyl extraction mechanism.

**1. Polarity and Surface Activity of TBP.** Properly describing the neat oil/water interfaces is a prerequisite prior to modeling the assisted uranyl transfer process. With the different TBP models, it is clear that TBP is surface active, with modulations, although, regarding the interface roughness, its covering by TBPs and the rate of exchange with the bulk oil phase. The thermodynamics of TBP has been studied experimentally at the water/dodecane interface by Sagert et al.[79,80] According to these authors, the standard free energy of transfer from water to oil ($\Delta G_{WO}$ = −4.8 kcal/mol) is mainly of entropic origin ($T\Delta S$ = −11.2 kcal/mol), while the enthalpic component is unfavorable ($\Delta H_{WO}$ = +6.4 kcal/mol), as expected for hydrophobic species. Furthermore, at small TBP mole fractions (up to $2.7 \times 10^{-4}$ in dodecane), a free energy of adsorption of 8.6 kcal/mol has been estimated. When compared to these $\Delta G_{WO}$ and $\Delta G_{OI}$ values, our calculated PMF results are in better agreement with SET1 than with SET5 or SET7 TBP models ($\Delta A_{WO}$ = −3.8, −8.6, and −9.4 kcal/mol, respectively). The affinity for the interface calculated in this series ($\Delta A_{IO}$ = 8.2, 4.5, and 3.0 kcal/mol, respectively) is also best represented with the SET1. Thus, although SET1 exaggerates the TBP interactions with $H_2O$, $HNO_3$ or $UO_2(NO_3)_2$ species in the gas phase, it better accounts for the thermodynamics of TBP at the aqueous (TIP3P) interface, presumably because the TIP3P water polarity is also exaggerated at the interface. On the other hand, the POL model using POL3 water somewhat underestimates the hydrophilicity and surface activity of TBP ($\Delta A_{WO}$ = −7.2 and $\Delta A_{IO}$ = 2.6 kcal/mol), suggesting that the SET5 charges, although satisfactorily accounting for the TBP interaction with $H_2O$ in the gas phase (Table S4) somewhat underestimate the corresponding interactions in solution (see also next section). What happens with other water and TBP model combinations (including polarizable ones) remains to be investigated.

The interfacial tension $\gamma$ is another relevant thermodynamic parameter. It decreases with the TBP affinity for the interface, and thus with the TBP charges (see Table S10): at "infinite dilution" (with a single TBP at the interface), $\gamma$ is similar with the different TBP models ($\gamma$ = 41 - 46 mN/m) and close to the experimental value of 50 mN/m for the hexane/water interface.[81] When TBP gets more concentrated, $\gamma$ decreases in the order $\gamma$(SET7) > $\gamma$(SET5) > $\gamma$(SET1), i.e., when TBP gets more polar and amphiphilic. For instance, $\gamma$ = 40, 23, and 14 mN/m, respectively for the 1.1 M TBP solution, and $\gamma$ = 33, 10, and 2 mN/m, respectively for the pure-TBP/water interface. The SET5 result is close to the experimental value (8 mN/m[82]), while $\gamma$(SET1) is too low.

**2. TBP Polarity and Water (+ acid) Extraction.** In none of the simulated systems does TBP migrate to the bulk water phase, in keeping with its low experimental solubility in water ($\approx 10^{-3}$ mol/L).[83] On the other hand, some water solubilizes in the oil phase, by a decreasing amount when TBP gets less polar, in the order SET1 > SET5 > SET7 for the pure-TBP/water and TBP+hexane/water systems. The number of "extracted" $n(H_2O)_{oil}$ water molecules (beyond 5 Å from the Gibbs surface) and corresponding $[H_2O]_{oil}$ concentrations after 5 ns (or additional 1 ns at 400K + 5 ns at 300 K to further equilibrate some systems) are summarized in Table S11. When compared to the experimentally reported values, the humidity of the oil phase is generally exaggerated with the SET1, underestimated with the SET5, and a fortiori SET7 TBP models without polarization.

For example, for the pure-TBP/water system, $[H_2O]_{oil} \approx$ 6.16, 0.61, and 0.05 mol/L, respectively, in the SET1, SET5, and SET7 series after 5 + 1+5 ns (exp. ≈ 2.6 mol/L).[83] When TBP gets diluted in hexane (1.1 M TBP solution) it extracts less water than does pure-TBP: $[H_2O]_{oil} \approx$ 1.08, 0.14, and 0.00 mol/L, respectively with the three models (exp. ≈ 0.3 mol/L). In the corresponding acidic conditions: $[H_2O]_{oil} \approx$ 0.75, 0.09, and 0.00 mol/L, respectively (exp. ≈ 0.3 mol/L).[75]

The effects of polarization on water extraction are much smaller than those of the TBP charges. In fact, the POL3 water molecule is intrinsically less polar than its TIP3P analogue and hence more easily transferred from the interface to the oil phase; on the other hand, it forms weaker H-bonds with TBP in the organic phase (see Table S4). The overall result is that the oil phase gets somewhat more humid with polarization (POL model with SET5 charges) than without (SET5 NO-POL). For instance, in the "pure TBP" phase $[H_2O]_{oil} \approx$ 0.47 and 0.35 mol/L, respectively, while in the 1.1 M TBP phase,


dx.doi.org/10.1021/jp411332e | J. Phys. Chem. B 2014, 118, 3133−3149

$[H_2O]_{oil}$ ≈ 0.08 and 0.05 mol/L, respectively. For the corresponding acidic systems, $[H_2O]_{oil}$ ≈ 0.23 and 0.07 mol/L, respectively. With polarization and SET5-TBP, the humidity of the oil phase remains somewhat lower than experiment. On the other hand, with the SET1-TBP model, the humidity is exaggerated with or without polarization (for instance, $[H_2O]_{oil}$ ≈ 3.5 mol/L with both models in pure TBP).

In acidic systems, some nitric acid is also extracted, always in the neutral form $HNO_3$, while the $H_3O^+$ and $NO_3^-$ ions remain in water, which is consistent with experimental reports.[84] The amounts of extracted acid to a 1.1 M TBP solution are given in Table S11. As for water, the final $[HNO_3]_{oil}$ concentrations (in mol/L) decrease in the order SET1 (0.23) > SET5 (0.17) > SET7 (0.08). All are lower than the experimental value (0.56 mol/L),[75] because in the case of SET1-TBP nearly all $HNO_3$ species initially present in water (17 among 20) have migrated to the oil phase, limiting further acid extraction without recombination (from $H_3O^+$ $NO_3^-$ to $HNO_3$), a feature precluded by the force field approach. Furthermore, with SET5 or SET7 charges, the acid attraction by TBP is somewhat underestimated.

**3. On the (Lack of) Surface Activity of the Uranyl Complex. Implications for the Extraction Mechanism.** The simulations with the different TBP and solvent models show that the aqueous and oil phases do not mix at the microscopic level, and delineate interfaces onto which TBP's adsorb, concentrate, favoring cation complexation by a least motion pathway at the interface. Regarding uranyl nitrate, it is almost totally dissociated in water, but the proportion of $UO_2(NO_3)^+$ and $UO_2(NO_3)_2$ adducts increases with the nitric acid concentration[85] and with the proximity to the interface (its lower dielectric constant and polarity, compared to bulk water, yields a higher proportion of contact ion pairs). Likewise, nitric acid is less dissociated at the interface than in bulk water.[86] The neutral $UO_2(NO_3)_2$ species should thus approach more closely the interface than do the $UO_2(NO_3)^+$ or $UO_2^{2+}$ hydrated cations, facilitating their complexation with interfacial TBP's. Although the detailed sequence of TBP and nitrate coordination to uranyl cannot be established, our PMF results on $UO_2(NO_3)_2$ and $UO_2^{2+}$ transfer make clear that the $UO_2(NO_3)_2(TBP)_2$ complex forms "right at the interface".

The surface activity of the $UO_2(NO_3)_2(TBP)_2$ complex has not been, to our knowledge, evidenced by experiments. On the simulation side, nearly all previous MD and PMF reports indicated that this complex should be more surface active than TBP itself. In such a case, migration to the oil phase would be promoted by the accumulation of the complexes at the interface, lowering the interfacial tension. Our results do not support this view. According to the PMF simulations, the neutral complexes are surface active only when their ionic components are modeled with integer charges, whatever the tested TBP charges. With more appropriate ESP charges on the $UO_2(NO_3)_2$ moiety or on the whole complex, the latter is no more surface active. This feature is consistent with the MD study of Ye et al.[41] who observed migration of a $UO_2(NO_3)_2(TBP)_2(H_2O)$ complex from the interface to the oil phase, when the complex was modeled with adapted ESP charges. In the oil phase, this complex released water to form $UO_2(NO_3)_2(TBP)_3$ that was proposed as precursor of the $UO_2(NO_3)_2(TBP)_2$ extracted complex. On the other hand, when the dynamics started with "naked" $UO_2^{2+}$ and $NO_3^-$ ions (thus bearing integer charges), complexes of general formula $UO_2^{2+}(NO_3^-)_n(TBP)_m(H_2O)_k$ (with monodentate nitrates and $n + m + k = 5$) formed and remained near the interface without being extracted after 16 ns of dynamics.[87] These features are consistent with our PMF results on the lack of neither $UO_2(NO_3)_2$ nor $UO_2^{2+}$ extraction by TBP when uranyl is +2 charged.

Comparing the POL to NO-POL simulation results, we find no marked difference regarding the (lack of) surface activity of the complex depicted with $UN_{ESP}$/SET5 charges: the corresponding PMF curves look similar (no minimum at the interface). Further support comes from unconstrained MD simulations that started with five complexes near the interface (see Figure S26): within 5 ns of dynamics, most of them exchange between the bulk oil phase and the oil side of the interface, without being solvated by interfacial water (see color coded trajectories in Figures S26 and S28). Similar features are observed after mixing−demixing simulations of the same solution, with either NO-POL or POL models (see Figure S29).

**4. On the Importance of Ion−Counterion Combination and of Related Electronic Redistribution.** To retain the neutrality of the source and receiving phases, the cation's charge must be compensated by counterions, and this neutralization process most likely occurs at the interface.[88] As pointed out for liquid−liquid phase transfer catalytic systems,[28] cation−anion combination promotes the extraction process. It also induces charge redistributions that critically contribute to drive the cation toward the interface where it can interact with extracting ligands. The harder and more charged the ions, the highest are the charge transfer (plus polarization) effects within the ion pair and with surrounding water or ligands.[45,89] Here, $UO_2(NO_3)_2$ is found to be less hydrophilic and thus more "surface active" with $UN_{ESP}$ than with $UN_{integer}$ models. This feature is visible in the PMF simulations on $UO_2(NO_3)_2$ across the SET5-TBP+hexane/water interface (Figure 10): the free energy profile from the interface (I position, where the salt is not complexed by TBPs) to bulk water is nearly flat with the $UN_{integer}$ model, but rises (by ≈5.5 kcal/mol) with the $UN_{ESP}$ model. Similar features are observed without TBP and at higher salt concentration (with 5 $UO_2(NO_3)_2$ per box, corresponding to a ca. 0.15 M concentration; see Figure 11): a free energy minimum is observed near the interface with the $UN_{ESP}$ model ($\Delta A_{IW}$ ≈ 3 kcal/mol), but not with the $UN_{integer}$ one. Another distinguishing feature concerns the "supramolecular" arrangement of the $UO_2(NO_3)_2$ species: with the $UN_{integer}$ charges, they tend to aggregate in water, while with $UN_{ESP}$ charges they adsorb and "dilute" at the interface (see Figure S30), calling for further investigations on the surface behavior of uranyl nitrate and related ion pairing features using, for instance, CP-MD based approaches.[78,90,91]

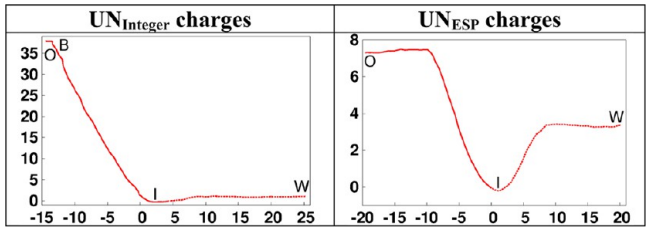


**Figure 11.** Interface crossing by $UO_2(NO_3)_2$, from hexane to neutral water (0.15 M "concentrated" solution containing 5 $UO_2(NO_3)$ species per box; system **P**): free energy profile ($\Delta A$ in kcal/mol). Typical snapshots are given in Figure S30.


dx.doi.org/10.1021/jp411332e | J. Phys. Chem. B 2014, 118, 3133−3149

**5. The Case of Uranyl Extraction by Other Neutral Hydrophobic Ligands (Amides).** The importance of ions representation on the surface activity of the extracted complex discussed above led us to question how general this feature is for other systems, especially when counterions are coordinated to the extracted metal. We recently studied by MD and PMF simulations the case of uranyl extraction by fatty amide ligands DEHiBA (*N,N*-di(2-ethylhexyl)isobutyramide), using integer charges on uranyl and nitrate, and found that the $UO_2(NO_3)_2(DEHiBA)_2$ complex adsorbs at the DEHiBA +hexane/water interface.[66] This led us to reconsider this PMF, using $UN_{ESP}$ instead of $UN_{integer}$ charges. The new results (Figure 12) reveal similar features as for the TBP complex, namely, the lack of energy minimum at the interface with the ESP model. This implies that the amide complexes, once formed at the interface, are not adsorbed but diffuse "freely" to the oil phase. Furthermore, the interface is not fully covered by the complexes, facilitating exchanges with the oil phase. Thus, as with the TBP ligands, the simulated interfacial landscape upon ion extraction markedly depends, among others, on the electrostatic representation of extracted ions in their free and complexed states.

## CONCLUSION

We have investigated interfacial features of model solutions involved in the uranyl complexation and extraction by TBPs, comparing different TBP models, of uranyl nitrates and, in selected cases, simulations with versus without polarization on all atoms. Among the tested parameters, the most critical one is the charge representation of the extracted ions, in conjunction with a reasonable choice of TBP charges. When ions are modeled with integer charges, extraction of $UO_2(NO_3)_2$ is predicted to be unfavored, while the preformed $UO_2(NO_3)_2(TBP)_2$ complexes adsorb and concentrate at the interface. Mimicking charge transfer and polarization effects in the $UO_2(NO_3)_2$ moiety or in the whole complex (here, via ESP charges) yields different views. First, the complexes are no more surface active. Second, along a PMF simulation with ESP charges, $UO_2(NO_3)_2$ spontaneously forms $UO_2(NO_3)_2(TBP)_2$ at the interface, followed by its energetically favorable transfer to the oil phase. Polarization effects somewhat reduce the surface activity of TBP, but have little influence on the interfacial behavior of its complex. The resulting picture of the interface "in action" thus involves a dynamic equilibrium where TBPs exchange between the bulk oil phase and the interface, while complexes formed at the interface diffuse "freely" to the oil phase, without accumulating in an interfacial layer. Similar features are expected for metal extraction by neutral ligands. Regarding the uranyl nitrate salt, the comparison of PMF results obtained with $UO_2(NO_3)_2$ and with the "naked" $UO_2^{2+}$ cation point to the key role of cation−anion combination (and related electronic reorganization) to promote the extraction process. Beyond the important studied case, our simulation results, combined with experimental results (for instance the time evolution of the surface tensions and spectroscopic signature[92,93]) should contribute to better understand what happens when ions cross water/oil interfaces.[3,4,7]

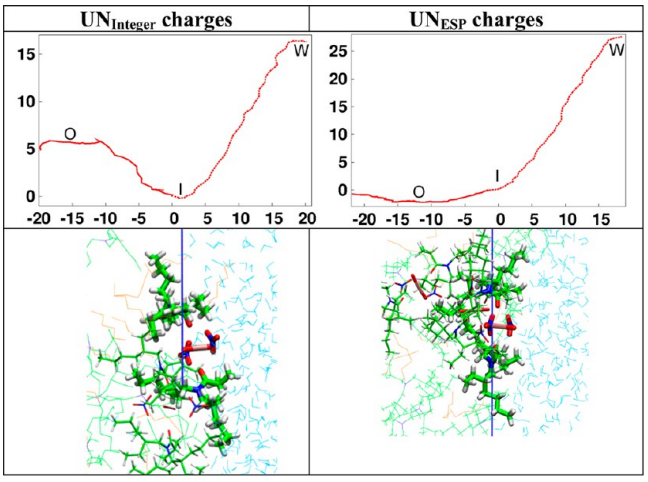


**Figure 12.** Interface crossing by the $UO_2(NO_3)_2(DEHiBA)_2$ complex, from the oil phase (hexane +40 DEHiBA + 4 complexes) to neutral water, with Integer versus ESP charges on uranyl nitrate: free energy profiles ($\Delta A$ in kcal/mol) and snapshots at the interface (I position). Snapshots at the O and W positions are given in Figure S31.

## ASSOCIATED CONTENT

### Supporting Information

Tables S1−S11 with atomic charges and polarizabilities, tests on QM versus AMBER interaction energies, energy components analysis, solvation features of O(TBP) and surface tensions. Figures S1 to S31 include snapshots of all simulated biphasic systems, density curves, water surface, snapshots along the PMF trajectories and views of cumulated trajectories, analysis of dipole moments of uranyl nitrate along the PMFs, PMF results for $UO_2^{2+}$ across the interface, and results of mixing-demixing simulations. This information is available free of charge via the Internet at http://pubs.acs.org.

## AUTHOR INFORMATION

### Corresponding Author

*E-mail: wipff@unistra.fr.

### Notes

The authors declare no competing financial interest.

## ACKNOWLEDGMENTS

The authors are grateful to IDRIS, CINES and Université de Strasbourg for computer resources, and to Etienne Engler, Alain Chaumont and Rachel Schurhammer for assistance and discussions. Support from the ANR ILLA (ANR-12-BS08-0021-03) is also acknowledged. G.W. is grateful to Jeanne, Noemie, Mathilde, and Nathan for their lively and stimulating questions.

## REFERENCES

(1) Watarai, H. What's Happening at the Liquid−Liquid Interface in Solvent Extraction Chemistry? *Trends in Analytical Chem.* **1993**, *12*, 313−318.

(2) Rydberg, J.; Cox, M.; Musikas, C.; Choppin, G. R. *Solvent Extraction. Principles and Practice*, 2nd ed., revised and expanded.; M. Dekker: New York, 2004.

(3) Watarai, H.; Teramae, N.; Sawada, T. *Interfacial Nanochemistry. Molecular Science and Engineering at Liquid-Liquid Interfaces*; Kluwer Academic Plenum: New York, 2005.

(4) Girault, H. H.; Schiffrin, D. J. Electrochemistry of Liquid−Liquid Interfaces. In *Electroanalytical Chemistry*; Bard, A. J., Ed.; Dekker: New York, 1989; Vol. *15*, pp 1−141.

(5) Starks, C. M.; Liotta, C. L.; Halpern, M. *Phase Transfer Catalysis*; Chapmann and Hall: New York, 1994.

(6) Volkov, A. G.; Deamer, D. W.; Tanelian, D. L.; Markin, V. S. *Liquid Interfaces in Chemistry and Biology*; John Wiley & Sons, Inc.: New York, 1998.
(7) Volkov, A. G.; Brevet, P. F. *Liquid Interfaces in Chemical, Biological and Pharmaceutical Applications. Non linear Optics at Liquid/Liquid Interfaces.*; M. Dekker: New York, 2001.
(8) Choppin, G. R. Complexation of Metal Ions. In *Principles of Solvent Extraction*; Rydberg, J., Musikas, C., Choppin, G. R., Eds.; M. Dekker: New York, 1992, pp 71−100.
(9) Musikas, C.; Schulz, W. W. Solvent Extraction in Nuclear Science and Technology. In *Principles and Practices of Solvent Extraction*; Rydberg, J., Musikas, C., Choppin, G. R., Eds.; M. Dekker, Inc.: New York, 1992; Chapter 11, pp 413−447.
(10) Condamines, N.; Musikas, C. The Extraction by *N,N*-dialkylamides. II. Extraction of Actinide Cations. *Solvent Extr. Ion Exch.* **1992**, *10*, 69−100.
(11) Hahn, H. T. The Mechanism of Uranium Extraction by Tributyl Phosphate. *J. Am. Chem. Soc.* **1957**, *79*, 4625−4629.
(12) Baumgärtner, F.; Finsterwalder, L. On the Transfer Mechanism of Uranium(VI) and Plutonium(IV) Nitrate in the System Nitric Acid−Water/Tributylphosphate−Dodecane. *J. Phys. Chem.* **1970**, *74*, 108−112.
(13) Lewis, J. B. An Interfacial Barrier Observed during Liquid−Liquid Extraction of Uranyl Nitrate. *Nature* **1956**, *178*, 274−275.
(14) Nitsch, W. The Concept of Interfacial Reactions for Mass-Transfer in Liquid/Liquid-Systems. *Faraday Discuss. Chem. Soc.* **1984**, *77*, 85−96.
(15) Horner, D.; Mailen, J.; Thiel, S.; Scott, T.; Yates, R. Interphase Transfer Kinetics Of Uranium Using The Drop Method, Lewis Cell, And Kenics Mixer. *Ind. Eng. Chem. Fundam.* **1980**, *19*, 103−109.
(16) Watarai, H.; Satoh, K. Kinetics of the Interfacial Mechanism in the Extraction of Nickel(II) with 5-Nonylsalicylaldoxime. *Langmuir* **1994**, *10*, 3913−3915.
(17) Nitsch, W. The Concept of Interfacial Reactions for Mass Transfer in Liquid/Liquid Systems. *Faraday Discuss. Chem. Soc.* **1983**, *77*, 85−96.
(18) Perera, J. M.; McCulloch, J. K.; Murray, B. S.; Grieser, F.; Stevens, G. W. An Attenuated Total Internal Reflection Spectroscopy Study of the Kinetics of Metal Ion Extraction at the Decane−Aqueous Solution Interface. *Langmuir* **1992**, *8*, 366−368.
(19) McCulloch, J. K.; Perera, J. M.; White, L. R.; Stevens, G. W.; Grieser, F. Direct Spectroscopic Measurement and Theoretical Modeling of the Diffusion of a Single Species in a Two-Phase Unstirred System. *J. Colloid Interface Sci.* **1996**, *184*, 399−405.
(20) Hokura, A.; Perera, J. M.; Grieser, F.; Stevens, G. W. A Kinetic Study of Nickel Ion Extraction by KELEX 100 at the Liquid−Liquid Interface. *Solvent Extr. Ion Exch.* **1998**, *16*, 619−636.
(21) Yamada, M.; Perera, J. M.; Grieser, F.; Stevens, G. W. A Kinetic Study of Copper Ion Extraction by P50 at the Water−Oil Interface. *Anal. Sci.* **1998**, *14*, 223−227.
(22) Yagodin, G. A.; Tarasov, V. V. Interfacial Phenomena in Liquid−Liquid Extraction. *Solvent Extr. Ion Exch.* **1984**, *2*, 139−179.
(23) McFearin, C. L.; Beaman, D. K.; Moore, F. G.; Richmond, G. L. From Franklin to Today: Toward a Molecular Level Understanding of Bonding and Adsorption at the Oil−Water Interface. *J. Phys. Chem. C* **2009**, *113*, 1171−1188.
(24) Martin-Gassin, G.; Gassin, P. M.; Couston, L.; Diat, O.; Benichou, E.; Brevet, P. F. Second Harmonic Generation Monitoring of Nitric Acid Extraction by a Monoamide at the Water−Dodecane Interface. *Phys. Chem. Chem. Phys.* **2011**, *13*, 19580−19586.
(25) Benjamin, I. Molecular Structure and Dynamics at Liquid−Liquid Interfaces. *Annu. Rev. Phys. Chem.* **1997**, *48*, 407−451.
(26) Berny, F.; Schurhammer, R.; Wipff, G. Distribution of Hydrophilic, Amphiphilic and Hydrophobic Ions at a Liquid−Liquid Interface: A Molecular Dynamics Investigation. *Inorg. Chim. Acta* **2000**, *300*−*302*, 384−394.
(27) Luo, G.; Malkova, S.; Yoon, J.; Schultz, D. G.; Lin, B.; Meron, M.; Benjamin, I.; Vanysek, P.; Schlossman, M. L. Ion Distributions near a Liquid−Liquid Interface. *Science* **2006**, *311*, 216−218.
(28) Benjamin, I. Recombination, Dissociation, and Transport of Ion Pairs across the Liquid/Liquid Interface. Implications for Phase Transfer Catalysis. *J. Phys. Chem. B* **2013**, *117*, 4325−4331.
(29) Wipff, G.; Lauterbach, M. Complexation of Alkali Cations by Calix[4]crown Ionophores: Conformation and Solvent Dependent $Na^+/Cs^+$ Binding Selectivity: A MD FEP Study. *Supramol. Chem.* **1995**, *6*, 187−207.
(30) Troxler, L.; Wipff, G. Interfacial Behaviour of Ionophoric Systems: Molecular Dynamics Studies on 18-crown-6 and its Complexes at the Water−Chloroform Interface. *Anal. Sci.* **1998**, *14*, 43−56.
(31) Sieffert, N.; Chaumont, A.; Wipff, G. Importance of the Liquid−Liquid Interface in Assisted Ion Extraction: New Molecular Dynamics Studies of Cesium Picrate extraction by a Calix[4]arene. *J. Phys. Chem. C* **2009**, *113*, 10610−10622.
(32) Chaumont, A.; Wipff, G. Polyoxometallates Keggin Anions at Aqueous Interfaces with Organic Solvents, Ionic Liquids and Graphite: A Molecular Dynamics Study. *J. Phys. Chem. C* **2009**, *113*, 18233−18243.
(33) Chaumont, A.; Wipff, G. Strontium Nitrate Extraction to Ionic Liquids by a Crown Ether: A Molecular Dynamics Study of Aqueous Interfaces with $C_4mim^+$ versus $C_8mim^+$ Based Ionic Liquids. *J. Phys. Chem. B* **2010**, *114*, 13773−13785.
(34) Beudaert, P.; Lamare, V.; Dozol, J.-F.; Troxler, L.; Wipff, G. Theoretical Studies on Tri-*n*-Butyl Phosphate: MD Simulations in Vacuo, in Water, in Chloroform and at a Water/Chloroform Interface. *Solvent Extr. Ion Exch.* **1998**, *16*, 597−618.
(35) Baaden, M.; Berny, F.; Wipff, G. The Chloroform/TBP/Aqueous Nitric Acid Interfacial System: A Molecular Dynamics Investigation. *J. Mol. Liq.* **2001**, *90*, 3−12.
(36) Baaden, M.; Berny, F.; Muzet, N.; Troxler, L.; Wipff, G., Interfacial Features of Assisted Liquid-Liquid Extraction of Uranyl and Cesium Salts: A Molecular Dynamics Investigation. In *Calixarenes for Separation*; ACS Symposium Series 757; Lumetta, G., Rogers, R., Gopalan, A., Eds.; ACS: Washington, DC, 2000; pp 71−85.
(37) Baaden, M.; Burgard, M.; Wipff, G. TBP at the Water−Oil Interface: The Effect of TBP Concentration and Water Acidity Investigated by Molecular Dynamics Simulations. *J. Phys. Chem. B* **2001**, *105*, 11131−11141.
(38) Baaden, M.; Berny, F.; Muzet, N.; Schurhammer, R.; Troxler, L.; Wipff, G. Separation of $Cs^+$ and $UO_2^{2+}$ Cations by Liquid−Liquid Extraction: Computer Simulations of the Demixing of Water/Oil Binary Solutions. In *Euradwaste 1999: Radioactive Waste Management Strategies and Issues*; Davies, C., Ed.; European Commission: Brussels, 2000; Vol. EUR 19143 EN, pp 519−522.
(39) Baaden, M.; Schurhammer, R.; Wipff, G. Molecular Dynamics Study of the Uranyl Extraction by Tri-*n*-butylphosphate (TBP): Demixing of Water/"Oil"/TBP Solutions with a Comparison of Supercritical $CO_2$ and Chloroform. *J. Phys. Chem. B* **2002**, *106*, 434−441.
(40) Jayasinghe, M.; Beck, T. L. Molecular Dynamics Simulations of the Structure and Thermodynamics of Carrier-Assisted Uranyl Ion Extraction. *J. Phys. Chem. B* **2009**, *113*, 11662−11671.
(41) Ye, X.; Cui, S.; deAlmeida, V. F.; Hay, B. P.; Khomami, B. Uranyl Nitrate Complex Extraction into TBP/Dodecane Organic Solutions: A Molecular Dynamics Study. *Phys. Chem. Chem. Phys.* **2010**, *12*, 15406−15409.
(42) Cui, S.; de Almeida, V. F.; Hay, B. P.; Ye, X.; Khomami, B. Molecular Dynamics Simulation of Tri-*n*-butyl-Phosphate Liquid: A Force Field Comparative Study. *J. Phys. Chem. B* **2012**, *16*, 305−313.
(43) Schurhammer, R.; Wipff, G. Effect of the TBP and Water on the Complexation of Uranyl Nitrate and the Dissolution of Nitric Acid into Supercritical $CO_2$ . A Theoretical Study. *J. Phys. Chem. A* **2005**, *109*, 5208−5216.
(44) Kohagen, M.; Brehm, M.; Thar, J.; Zhao, W.; Müller-Plathe, F.; Kirchner, B. Performance of Quantum Chemically Derived Charges and Persistence of Ion Cages in Ionic Liquids. A Molecular Dynamics Simulations Study of 1-*n*-Butyl-3-methylimidazolium Bromide. *J. Phys. Chem. B* **2011**, *115*, 693−702.

(45) Pluhařová, E.; Mason, P. E.; Jungwirth, P. Ion Pairing in Aqueous Lithium Salt Solutions with Monovalent and Divalent Counter-Anions. *J. Phys. Chem. A* **2013**, *117*, 11766−11773.
(46) Chang, T. M.; Dang, L. X. Molecular Dynamics Simulations of $CCl_4$−$H_2O$ Liquid-Liquid Interface with Polarizable Potential Models. *J. Chem. Phys.* **1995**, *104*, 6772−6783.
(47) Chang, T.-M.; Dang, L. X. Recent Advances in Molecular Simulations of Ion Solvation at Liquid Interfaces. *Chem. Rev.* **2005**, *106*, 1305−1322.
(48) Jungwirth, P.; Tobias, D. J. Ions at the Air/Water Interface. *J. Phys. Chem. B* **2002**, *106*, 6361−6373.
(49) Duvail, M.; Ruas, A.; Venault, L.; Moisy, P.; Guilbaud, P. MD Studies of Concentrated Binary Aqueous Solutions of Lanthanide Salts: Structure and Exchange Dynamics. *Inorg. Chem.* **2010**, *49*, 519−530.
(50) Bedrov, D.; Borodin, O.; Li, Z.; Smith, G. D. Influence of Polarization on Structural, Thermodynamic, and Dynamic Properties of Ionic Liquids Obtained from Molecular Dynamics Simulations. *J. Phys. Chem. B* **2010**, *114*, 4984−4997.
(51) Salanne, M.; Madden, P. A. Polarization Effects in Ionic Solids and Melts. *Mol. Phys.* **2011**, *109*, 2299−2315.
(52) Lauterbach, M.; Engler, E.; Muzet, N.; Troxler, L.; Wipff, G. Migration of Ionophores and Salts through a Water−Chloroform Liquid−Liquid Interface: Computer MD-PMF Investigations. *J. Phys. Chem. B* **1998**, *102*, 225−256.
(53) Valente, M.; Sousa, S. F.; Magalhães, A. L.; Freire, C. Transfer of the $K^+$ Cation Across a Water/Dichloromethane Interface: A Steered Molecular Dynamics Study with Implications in Cation Extraction. *J. Phys. Chem. B* **2012**, *116*, 1843−1849.
(54) Benay, G.; Wipff, G. Oil-Soluble and Water-Soluble BTPhens and their Europium Complexes in Octanol/Water Solutions: Interface Crossing Studied by MD and PMF Simulations. *J. Phys. Chem. B* **2013**, *117*, 1110−1122.
(55) Case, D. A.; Darden, T. A.; Cheatham, T. E., III; Simmerling, C. L.; Wang, J.; Duke, R. E.; Luo, R.; Crowley, M.; Walker, R. C.; Zhang, W. et al. *AMBER10*; University of California: San Francisco, CA, 2008.
(56) Cornell, W. D.; Cieplak, P.; Bayly, C. I.; Gould, I. R.; Merz, K. M.; Ferguson, D. M.; Spellmeyer, D. C.; Fox, T.; Caldwell, J. W.; Kollman, P. A. A Second Generation FF for the Simulation of Proteins, Nucleic Acids, and Organic Molecules. *J. Am. Chem. Soc.* **1995**, *117*, 5179−5197.
(57) Jorgensen, W. L.; Chandrasekhar, J.; Madura, J. D.; Impey, R. W.; Klein, M. L. Comparison of Simple Potential Functions for Simulating Liquid Water. *J. Chem. Phys.* **1983**, *79*, 926−936.
(58) Jorgensen, W. L.; Tirado-Rives, J. The OPLS Potential Functions for Proteins. Energy Minimizations for Crystals of Cyclic Peptides and Crambin. *J. Am. Chem. Soc.* **1988**, *110*, 1657−1666.
(59) Guilbaud, P.; Wipff, G. Force Field Representation of the $UO_2^{2+}$ Cation from Free Energy MD Simulations in Water. Tests on Its 18-Crown-6 and $NO_3^-$ Adducts, and on Its Calix[6]arene$^{6-}$ and CMPO Complexes. *J. Mol. Struct. (THEOCHEM)* **1996**, *366*, 55−63.
(60) Rai, N.; Tiwari, S.; Maginn, E. J. Force Field Development for Actinyl Ions via Quantum Mechanical Calculations: An Approach to Account for Many Body Solvation Effects. *J. Phys. Chem.* **2012**, *116*, 10885−10897.
(61) Schurhammer, R.; Wipff, G., Uranyl Extraction by TBP from a Nitric Aqueous Solution to SC-$CO_2$: MD Simulations of Phase Demixing and Interfacial Systems., In *Separations and Processes Using Supercritical Carbon Dioxide*; Gopalan, A. S., Wai, C., Jacobs, H., Eds.; ACS: Washington, DC, 2003; Vol. *860*, Chapter 15, pp 223−244.
(62) Caldwell, J. W.; Kollman, P. A. Structure and Properties of Neat Liquids Using Nonadditive Molecular Dynamics: Water, Methanol, and *N*-Methylacetamide. *J. Phys. Chem.* **1995**, *99*, 6208−6219.
(63) Agostini, G.; Giacometti, G.; Clemente, D. A.; Vincentini, M. Crystal and Molecular Structure of Uranyl Nitrate Trimethylphosphate. *Inorg. Chim. Acta* **1982**, *62*, 237.
(64) York, D. M.; Darden, T. A.; Pedersen, L. G. The Effect of Long-Range Electrostatic Interactions in Simulations of Macromolecular Crystals: A Comparison of the Ewald and Truncated List Methods. *J. Chem. Phys.* **1993**, *99*, 8345−8348.
(65) Berendsen, H. J. C.; Postma, J. P. M.; van Gunsteren, W. F.; DiNola, A. Molecular Dynamics with Coupling to an External Bath. *J. Chem. Phys.* **1984**, *81*, 3684−3690.
(66) Benay, G.; Wipff, G. Liquid−Liquid Extraction of Uranyl by an Amide Ligand: Interfacial Features Studied by MD and PMF Simulations. *J. Phys. Chem. B* **2013**, *117*, 7399−7415.
(67) Kollman, P. Free Energy Calculations: Applications to Chemical and Biochemical Phenomena. *Chem. Rev.* **1993**, *93*, 2395−2417.
(68) Frisch, M. J.; Trucks, G. W.; Schlegel, H. B.; Scuseria, G. E.; Robb, M. A.; Cheeseman, J. R.; Scalmani, G.; Barone, V.; Mennucci, B.; Petersson, G. A. et al. *Gaussian 09*, revision B.01; Gaussian, Inc.: Wallingford, CT, 2010.
(69) Institut für Theoretische Chemie, Universität Stuttgart. ECPs and corresponding valence basis sets. www.theochem.uni-stuttgart.de.
(70) Johnson, W. F.; Dillon, R. L. *Physical Properties of Tributylphosphate-Diluent*, Report-29086; Hanford Atomic Products Operation: Richland, WA, 1953.
(71) Petkovic, D. M.; Kezele, B. A.; Rajic, D. R. Dipole Moments of Some Neutral Organic Phosphates. *J. Phys. Chem.* **1973**, *77*, 922−924.
(72) Estok, G. K.; Wendlandt, W. W. Electric Moments of Some Alkyl Phosphates and Thiophosphates. *J. Am. Chem. Soc.* **1955**, *77*, 4767−4769.
(73) Paloncyova, M.; Berka, K.; Otyepka, M. Convergence of Free Energy Profile of Coumarin in Lipid Bilayer. *J. Chem. Theory Comput.* **2012**, *8*, 1200−1211.
(74) Bühl, M.; Kabrede, H.; Diss, R.; Wipff, G. Effect of Hydration on Coordination Properties of Uranyl$^{(VI)}$ Complexes. A First-Principles Molecular Dynamics Study. *J. Am. Chem. Soc.* **2006**, *128*, 6357−6368.
(75) Hlushak, S. P.; Simonin, J. P.; Caniffi, B.; Moisy, P.; Sorel, C.; Bernard, O. Description of Partition Equilibria for Uranyl Nitrate, Nitric Acid and Water Extracted by Tributylphosphate in Dodecane. *Hydrometallurgy* **2011**, *109*, 97−105.
(76) Kerisit, S.; Liu, C. Structure, Kinetics, and Thermodynamics of the Aqueous Uranyl(VI) Cation. *J. Phys. Chem. A* **2013**, *117*, 6421−6432.
(77) Bühl, M.; Sieffert, N.; Chaumont, A.; Wipff, G. Water versus Acetonitrile Coordination to Uranyl. Effect of Chloride Ligands. *Inorg. Chem.* **2012**, *51*, 1943−1952.
(78) Bühl, M.; Wipff, G. Insights into Uranyl Chemistry from Molecular Dynamics Simulations. *ChemPhysChem* **2011**, *12*, 3095−3105.
(79) Sagert, N. H.; Lee, W.; Quinn, M. J. The Adsorption of Tri-*n*-Butylphosphate at the *n*-Dodecane-Water Interface. *Can. J. Chem.* **1979**, *57*, 1218.
(80) Sagert, N. H.; Lee, W. The Adsorption of Trialkylphosphates between Dodecane and Water. *Can. J. Chem.* **1980**, *58*, 1463−1467.
(81) Zeppieri, S.; Rodriguez, J.; deRamos, A. L. L. Interfacial Tension of Alkane + Water Systems. *J. Chem. Eng. Data* **2001**, *46*, 1086−1088.
(82) Schulz, W. W.; Navratil, J. D.; Kertes, A. S. *Science and Technology of Tributyl Phosphate*; CRC Press: Boca Raton, FL, 1984.
(83) Marcus, Y. *The Properties of Solvents*; John Wiley & Sons: Chichester, 1998; Vol. *4*.
(84) Naito, K.; Suzuki, T. The Mechanism of the Extraction of Several Proton Acids by TBP. *J. Phys. Chem.* **1962**, *66*, 983−988.
(85) Ye, X.; Smith, R. B.; Cui, S.; deAlmeida, V.; Khomami, B. Influence of Nitric Acid on Uranyl Nitrate Association in Aqueous Solutions: A Molecular Dynamics Simulation Study. *Solvent Extr. Ion Exch.* **2010**, *28*, 1−18.
(86) Soule, M. C. K.; Blower, P. G.; Richmond, G. L. Nonlinear Vibrational Spectroscopic Studies of the Adsorption and Speciation of Nitric Acid at the Vapor/Acid Solution Interface. *J. Phys. Chem. A* **2007**, *111*, 3349−3357.
(87) Ye, X.; Cui, S.; de Almeida, V.; Khomami, B. Interfacial Complex Formation in Uranyl Extraction by Tributyl Phosphate in Dodecane Diluent: A Molecular Dynamics Study. *J Phys. Chem. B.* **2009**, *113*, 9852−9862.

(88) Popov, A. N., Counterions and Adsorption of Ion-Exchange Extractants at the Water/Oil Interface. In *The Interface Structure and Electrochemical Processes at the Boundary between Two Immiscible Liquids*; Kazarinov, V. E., Ed.; Springer Verlag: Berlin, 1987; pp 179−205 and references cited therein.
(89) O'Brien, J. T.; Williams, E. R. Effect of Ions on Hydrogen Bonding Water Networks in Large Aqueous Nanodrops. *J. Am. Chem. Soc.* **2012**, *134*, 10228−10236.
(90) Pollet, R.; Marx, D. Ab initio Simulation of a Gadolinium Based Magnetic Resonance Imaging Contrast Agent in Aqueous Solution. *J. Chem. Phys.* **2007**, *126*, 181102.
(91) Terrier, C.; Vitorge, P.; Gaigeot, M.-P.; Spezia, R.; Vuilleumier, R. Density Functional Theory Based Molecular Dynamics Study of Hydration and Electronic Properties of Aqueous $La^{3+}$. *J. Chem. Phys.* **2010**, *133*, 044509.
(92) Martin-Gassin, G.; Gassin, P. M.; Couston, L.; Diat, O.; Benichou, E.; Brevet, P. F. Nitric Acid Extraction with Monoamide and Diamide Monitored by Second Harmonic Generation at the Water/Dodecane Interface. *Colloids Surf. A: Physicochem. Eng. Aspects* **2012**, *413*, 130−135.
(93) Haslam, S.; Croucher, S. G.; Hickman, C. G.; Frey, J. G. Surface Second Harmonic Generation Studies of the Dodecane/Water Interface: The Equilibrium and Kinetic Behaviour of *p*-Nitrophenol and tri-*n*-butyl Phosphate. *Phys. Chem. Chem. Phys.* **2000**, *2*, 3235−3245.